UILU-ENG-81-2012

CIVIL ENGINEERING STUDIES
STRUCTURAL RESEARCH SERIES NO. 493

INFLUENCE OF STIRRUP-TIE SHAPE ON INELASTIC CYCLIC RESPONSE OF FLANGED REINFORCED CONCRETE FLEXURAL MEMBERS

By
DALE R. WILHELM
and
CHARLES F. SCRIBNER

UNIVERSITY OF ILLINOIS
at URBANA-CHAMPAIGN
URBANA, ILLINOIS
AUGUST 1981

INFLUENCE OF STIRRUP-TIE SHAPE ON INELASTIC CYCLIC RESPONSE OF FLANGED REINFORCED CONCRETE FLEXURAL MEMBERS

by

Dale R. Wilhelm

and

Charles F. Scribner

University of Illinois
at Urbana-Champaign
Urbana, Illinois
August, 1981

50272-101

REPORT DOCUMENTATION PAGE	1. REPORT NO. UILU-ENG-81-2012	2.	3. Recipient's Accession No.

4. Title and Subtitle
Influence of Stirrup-Tie Shape on Inelastic Cyclic Response of Flanged Reinforced Concrete Flexural Members

5. Report Date
August 1981

6.

7. Author(s)
Dale R. Wilhelm and Charles F. Scribner

8. Performing Organization Rept. No.
SRS No. 493

9. Performing Organization Name and Address
University of Illinois at Urbana-Champaign
Urbana, IL 61801

10. Project/Task/Work Unit No.

11. Contract(C) or Grant(G) No.
(C)
(G)

12. Sponsoring Organization Name and Address
University of Illinois Engineering Experiment Station
Urbana, IL 61801

13. Type of Report & Period Covered

14.

15. Supplementary Notes

16. Abstract (Limit: 200 words)

Three reinforced concrete flanged sections (T-sections) having different shapes of shear reinforcement were subjected to cyclic inelastic flexure representative of what framed structure members might be forced to endure during a severe earthquake. The different types of shear reinforcement consisted of closed hoops and two types of U-shaped stirrups, neither having been supplemented with cap ties. This report documents the experimental work, presents data obtained during tests (including energy dissipation capacities) and discusses the implications of test results on possible changes in reinforcement details for frame structures in seismic regions.

17. Document Analysis a. Descriptors

Confinement, cyclic loading, earthquake response, flexure, framed structures, lateral reinforcement, shear strength, stirrups, T-sections.

b. Identifiers/Open-Ended Terms

c. COSATI Field/Group

18. Availability Statement	19. Security Class (This Report)	21. No. of Pages
Release Unlimited	UNCLASSIFIED	78
	20. Security Class (This Page) UNCLASSIFIED	22. Price

TABLE OF CONTENTS

LIST OF TABLES

LIST OF FIGURES

CHAPTER 1

INTRODUCTION

1.1 Object and Scope

The object of this test series was to examine the influence of stirrup-tie configurations on the behavior of reinforced concrete T-beams subjected to repeated reversed inelastic flexure. Three different tie shapes were used in construction of the three specimens tested. They were: (1) one-piece closed hoops conforming to current ACI Building Code (Ref. 1) seismic criteria, (2) U-shaped stirrups with vertical legs terminating in 180 degree standard hooks and with no cap ties, and (3) intentionally unconservative U-shaped stirrups in which vertical legs terminated in standard 90 degree hooks bent outward, or away from the beam core. These tests were designed to determine the possibility of using tie configurations which allow easy steel placement during construction of flanged sections or beams cast monolithically with slabs, but which do not decrease the seismic safety of these members.

Dimensions and longitudinal reinforcement ratios of the beams were chosen to produce maximum gross shear stresses of approximately $4\text{-}5\sqrt{f'_c}$ psi ($0.33\text{-}0.42\sqrt{f'_c}$ MPa) in all beams. Evaluation of specimen behavior was based on measurements of loads and deflections, steel strains, member energy dissipation, and general observations of crack patterns and concrete damage during testing.

1.2 Previous Investigations

Past research investigating the behavior of T-sections and the influence of differing stirrup-tie configurations on the behavior of reinforced concrete beams under repeated reversed loading has been limited.

Ma, Bertero, and Popov (2) did extensive studies on the behavior of reinforced concrete rectangular and T-shaped beams under repeated reversed loading, using one-piece closed ties in all their specimens. Among other considerations, they tested the effect of providing supplementary cross ties to support main longitudinal reinforcement not restrained by the corners of ties. Cross ties delayed the buckling of bars previously unrestrained by the corners of ties, improving beam core confinement and increasing beam shear resisting capacity.

Investigating the effects of varying stirrup configurations, Behera and Rajagopalan (3) used two-piece U-stirrups in one rectangular beam and in two L-shaped beams subjected to flexure, shear, and torsion (L-shaped beams only). They compared the behavior of these three beams with that of beams containing shear reinforcement consisting of one-piece closed hoops. Their results indicated that beams containing two-piece stirrups performed adequately under monotonic loading, but gave no prediction of expected performance of such beams under repeated reversed loading.

CHAPTER 2

OUTLINE OF EXPERIMENTAL PROGRAM

2.1 Description of Specimens

Three specimens were constructed for this investigation. Each specimen consisted of two flanged, or T-beam, portions joined to a central crossbeam section intended to represent the support conditions which might exist in an actual frame structure. The specimen chosen was not intended to model any particular prototype structure. Specimen plan and side views are shown in Fig. 2.1. The conditions of load application and support are idealized in Fig. 2.2. The positive sense of load and load point displacement was assumed to be upward, as shown in this figure.

Overall specimen dimensions and arrangement of longitudinal steel reinforcement were the same for all specimens. Longitudinal reinforcement consisted of #4, #7, and #9 bars, while shear reinforcement consisted of ties and stirrups bent from #3 bars. Temperature and shrinkage reinforcement, as required by the current ACI Building Code, consisted of #3 bars placed in the flange of the specimens at right angles to the longitudinal reinforcement. A typical beam cross section is shown in Fig. 2.3.

A typical section of the center crossbeam portion of the specimens is shown in Fig. 2.4. Crossbeam longitudinal reinforcement consisted of #9 bars while vertical reinforcement consisted of #3 stirrup-ties. The top longitudinal reinforcement of the crossbeam section was placed perpendicular to and below the longitudinal reinforcement in the flange of Specimen 1. The top longitudinal reinforcement of the crossbeam section was placed perpendicular to and above the longitudinal reinforcement in the flanges of Specimens 2 and 3.

2.2 Description of Transverse Reinforcement

The configuration of beam transverse reinforcement was the only test variable. The three tie configurations used in this investigation are shown in Fig. 2.5. Each of the three beams tested contained only one type of shear reinforcement in the regions of the beams which underwent inelastic flexure. Type I stirrups (used in Specimen 1) were closed hoops conforming to current ACI Building Code seismic criteria. Type IV stirrups (used in Specimen 2) were U-shaped. Vertical legs terminated in standard 180 degree hooks with 2 1/2 in. (64 mm) extensions past the bends. Type V stirrups (used in Specimen 3) were intentionally unconservative U-shaped stirrups in which the vertical legs terminated in 90 degree hooks bent outward, or away from the beam core, with ten bar diameter (3.75 in., 95 mm) extensions past the hooks. No cap ties were used in conjunction with Type IV or Type V stirrups. Stirrup spacing, which was the same for all three specimens and which conformed to ACI Building Code criteria for stirrups to be used in seismic zones, is shown in Fig. 2.6.

Original plans for testing had included an examination of the behavior of beams containing two additional shear reinforcement configurations which had been designated as Types II and III. The stirrups which had been intended for use in those beams were identical to the Type IV stirrups used in Specimen 2. These stirrups would have been supplemented with cap ties of two types. The performance of Specimen 2 was so nearly similar to that of Specimen 1, however, that testing of the influence of the two cap tie configurations was considered superfluous.

2.3 Fabrication and Material Properties

The wooden formwork used for the casting of the test specimens is shown in Fig. 2.7. Shear reinforcement and temperature steel were tied to the

longitudinal steel with 19 gauge wires. After the formwork had been oiled, the assembled steel reinforcement was placed on small concrete blocks in the forms. These blocks helped maintain the position of the reinforcement during the placement of the concrete. Steel tubes were used to form holes for the later attachment of the loading ram to the specimen. The formwork and steel cage for Specimen 2 prior to placement of concrete are shown in Fig. 2.8. A mechanical vibrator was used to consolidate concrete during placement. Standard 6 in. by 12 in. (152 mm by 305 mm) concrete cylinders were cast along with each test specimen.

Specimens and cylinders were cured under wet burlap and plastic sheeting for seven days, at which time the forms were removed. The specimens and cylinders were then cured uncovered in the laboratory until testing. Specimen and cylinder ages at testing are presented in Table 2.2.

A single concrete mix design was used in the construction of all specimens. The mix proportions, by dry weight, were 1.0:3.7:3.8 (cement: sand: 3/4 in. limestone). Type I cement was used with a water to cement ratio of 0.6:1.0.

Two batches of concrete were required for each specimen cast. All concrete was mixed in a Koehring Model 170 Cyclo-Mixer 1/2 cubic yard (0.38 m^3) capacity mixer. The first batch was placed in the region near the crossbeam section. The second batch was placed in the regions near the end supports. Measured compressive strengths, splitting strengths, and cylinder ages at the time of testing are presented in Table 2.2. Stress-strain relationships were measured for all concrete batches. Typical stress-strain curves are shown in Fig. 2.9.

Typical measured stress-strain relations for the four sizes of reinforcing steel used in the construction of each specimen are shown in

Fig. 2.10. Measured properties of all steels are summarized in Table 2.3.

2.4 Description of Test Setup

All specimens were attached to the Structural Laboratory floor at their end supports by high strength bolts and loaded with a servo-controlled, double-acting hydraulic ram which was supported by a separate frame. The supports of the specimen, consisting of 3 1/2 in. (89 mm) diameter pipes cast integrally with the specimen, were held by steel yokes welded to steel W-sections. The W-sections were in turn bolted to the laboratory floor. The east holding yoke was slotted to allow for longitudinal expansion of the specimen during the test. The test apparatus, with Specimen 1 in position, is shown in Fig. 2.11a.

For the testing of Specimen 1, the W-sections and holding yokes were bolted directly to the laboratory floor, as shown in Fig. 2.11a, and load point deflections were measured with respect to the floor. Deflections measured in this way included support motions, which were measured separately using dial gages. Details of support motion measurement are contained in the section of this report dealing with instrumentation.

For the testing of Specimens 2 and 3, concrete blocks were used to elevate the specimens and holding yokes. This allowed easier inspection of the specimens' ventral surface during the test. Load point deflections of Specimens 2 and 3 were measured with respect to the supports by using a measuring frame which was hung from the supports, as shown in Fig. 2.11b.

A 100 kip (445 kN) capacity hydraulic ram, visible in Fig. 2.11, was used to apply a vertical load to the specimen at the center of the crossbeam section. Because the ram was attached to both an external frame and to

the specimen by greased spherical connections, it was considered to impart no moment to the specimen at its point of attachment.

2.5 Testing Procedure

The intended pattern of deflection for all three specimens is shown in Fig. 2.12. Because the scope of the investigation was confined to examining the influence of stirrup shape on flanged section behavior, no attempt was made to subject the specimens to a load history corresponding to an actual earthquake, but rather to subject all specimens to approximately the same load history.

During the first eight cycles of loading, load point displacements varied from 1.5 to 3 percent of the beam shear span (measured from the face of the crossbeam section to the center of pin supports, shear span of each half of the total specimen was 50 in., 1270 mm), or from 0.75 to 1.5 in. (19 to 38 mm).

The ninth cycle of deflection was intended to determine member small-displacement stiffness remaining at this stage of testing, and deflection was limited to 1 percent of the shear span (0.5 in., 13 mm). Following application of the ninth load cycle, successively larger maximum displacements were imposed cyclically until the members failed.

The rationale for the load history was based on previous research and on the current beliefs of some members of the engineering community. Gosain, Brown, and Jirsa (4) have suggested that a "hinging region will provide adequate energy absorption if it can withstand five load cycles at five times the yield deflection," assuming capacity in each cycle of load remains as high as 75% of yield capacity. In addition, recent informal surveys of practicing engineers and designers indicate that maximum acceptable story drift during earthquakes should be limited to less than 3% of story

height. The load history chosen for the specimens discussed herein was believed to reasonably satisfy both these criteria, with the first eight cycles of load representing an upper bound of deformation requirement that could be realistically expected for a frame member during severe earthquake loading.

2.6 Instrumentation

Quantities measured at discrete intervals during each test were applied load, load point displacement, steel strains, and beam flexural rotation measured over an 8 in.(203 mm) section adjacent to crossbeam west face.

Applied load was measured with a 100 kip capacity load cell connected between the load ram and the specimen load point (the center of the crossbeam). Load point displacement and beam flexural rotation were measured with the LVDT's whose position is shown in Fig. 2.13.

The progress of each test was monitored by plotting applied load vs. load point displacement on an X-Y plotter. At selected times during the test, loading was temporarily halted to allow recording of measurements of ram load, LVDT positions, and strain gage and dial gage readings.

During the test of Specimen 1, load point displacement was measured with respect to the laboratory floor. The displacements measured in this manner included displacement due to support pin motion. To determine support displacement relative to the laboratory floor, four mechanical dial gages were positioned beneath the support pins as shown in Fig. 2.11a. Average support displacements measured at each cessation of loading were subtracted from load point displacement measurements to obtain true load point displacement with respect to the pin supports.

During the tests of Specimens 2 and 3, load point displacement with respect to the supports was measured directly by connecting LVDT #1 between the beam load point and the measuring frame as described previously. A mechanical dial gage was used in each test to verify the load point displacement as measured by LVDT #1.

The location of the strain gages used on selected longitudinal and transverse reinforcement is shown in Fig. 2.14. Strain gage #3 was used to measure transverse strain in the beam flange. It was attached to the top leg of the second stirrup-tie west of the crossbeam in Specimen 1 and to the side of the temperature steel at approximately the same location in Specimens 2 and 3.

Electrical impulses from the load cell, LVDT's, and strain gages were measured by a Vidar data acquisition system and recorded on paper tape for later processing and analysis by digital computer.

CHAPTER 3

OBSERVED BEHAVIOR

3.1 Introduction

Evaluation of specimen behavior was based on measurements of loads and displacements, member energy dissipation, steel strains, beam rotations, and general observations of crack patterns and concrete damage. These measurements and observations are presented and discussed in this chapter.

3.2 Load-Displacement Curves

Ram load vs. load point displacement relationships are shown in Fig. 3.1. Load vs. displacement curves for Specimen 1 have been corrected for support movements as described in the section of this report dealing with instrumentation. Positive load and positive displacement refer to negative beam curvature (hogging), or load ram tension.

Characteristics of specimen behavior evident in the load-displacement curves are as follows:

1) Initial elastic flexural stiffness of the specimens containing Type IV and Type V stirrups (Specimens 2 and 3) was slightly larger than the corresponding stiffness of the specimen containing Type I ties (Specimen 1). This was considered to result from the higher strength concrete in Specimens 2 and 3 as compared to that in Specimen 1, and from factors other than the type of shear reinforcement being used.

2) The overall flexural stiffness (slope of a line drawn between points of maximum positive and negative load on the load-displacement curve) of a member during a given load cycle was less than the corresponding stiffness during the previous load cycle. Specimen 3 was softened by the

large maximum displacement imposed during its first cycle of positive displacement and as a result its flexural stiffness during positive displacement was less than that of Specimens 1 and 2 for load cycles 2 through 6.

3) During all load cycles except the first, each specimen suffered loss of shear stiffness at small displacements from the original unloaded beam position, shown as "pinching" of the load-displacement curves. The pinching became more pronounced as loading progressed, indicating that beam cracking and deterioration were resulting in progressive loss of shear strength.

3.3 Energy Dissipation Measurements

The ability of the beams to dissipate energy during cyclic loading was considered to be a good indication of the durability of the specimens. Areas enclosed by the load-displacement curves (Fig. 3.1) were measured to determine the energy dissipation capacities of the members. Energy dissipation values for the three specimens, including total energy dissipation during the first eight load cycles and total energy dissipated by each specimen prior to failure, are presented in Table 3.1.

3.4 Steel Strain Relationships

In this section various relationships between ram load, load point displacement, and steel strains are presented. Positive strain refers to tensile strain in the steel.

Strain in longitudinal steel was measured by strain gages 4, 5, 6, and 7, the positions of which have been previously shown in Fig. 2.14.

Relationships between ram load and average strain measured in top and bottom longitudinal steel are shown in Figs. 3.2 and 3.3.

The relationships between load point displacement and steel strains in the vertical stirrup legs as measured by strain gages 1 and 2 are shown in Figs. 3.4 and 3.5. The location of these strain gages has been previously shown in Fig. 2.14. As indicated by strains measured by gage 2 in Specimen 3, strain in the vertical legs of this stirrup exceeded yield strain during the first loading cycle of Specimen 3. This resulted from the large positive load point displacement which was accidentally imposed on Specimen 3 during its first load cycle and not necessarily from the shape of the stirrup being used.

Relationships between load point displacement and transverse strain in the flange of the specimens as measured by strain gage 3 are presented in Fig. 3.6. The location of strain gage 3 has been previously discussed and is illustrated in Fig. 2.14. It was hoped that it would be possible to qualitatively relate transverse strain to the loss of confinement of the beam core. Observations regarding the character of transverse strains measured in the individual beams are as follows:

1) During any load cycle, the transverse strains measured during positive load point displacement were similar in magnitude to those measured during negative displacement for Specimens 1 and 2.

2) Transverse strains measured in Specimen 2 never reached the transverse steel yield strain and were generally less than those measured in Specimen 1.

3) Transverse strains accompanying positive beam curvature (sagging) were generally greater in Specimen 3 than in Specimen 2. Transverse strains

accompanying negative curvature (hogging) were similar in magnitude in Specimens 2 and 3.

4) The largest measured transverse strain was seen in Specimen 3 during positive curvature in the beam's tenth load cycle, indicating that the concrete flange was expanding laterally and losing its ability to provide lateral confinement to the top portion of the beam at that stage of loading.

3.5 Ram Load and Load Point Displacement vs. Beam Rotation

As previously described, the flexural rotation over an 8 in. (203 mm) length of the beam immediately west of the center crossbeam was measured by LVDT's 2 and 4. The quantitative utility of this measurement is not exceptional, as it is necessary to estimate a curvature distribution in order to compare actual and theoretical relationships of moment to curvature. The measurement is qualitatively useful, however, in determining the contribution of flexure and shear to total deformation during cyclic loading.

The relationships of ram load and load point displacement to the flexural rotation measured for the first eight cycles of loading are presented in Figs. 3.7 and 3.8. The dashed line representing the behavior of Specimen 3 in Fig. 3.7(c) was arrived at by estimation because of the previously discussed problem of load ram control during the test of that specimen. The following characteristics of member behavior are evident in these relationships.

(1) Maximum flexural rotations remained essentially constant for all members during all cycles having the same maximum displacements.

(2) The contribution of flexural rotation to total member deformation remained essentially constant for all deformation levels during the first eight cycles of loading of each member.

(3) The ratio of flexural rotation to total deformation was essentially constant for all members tested.

It may be inferred from these observations that because the contribution of flexure to total deformation remained constant, the contribution of shear strain to total deformation, both within and outside of the plastic hinging regions of the members remained essentially constant.

3.6 Crack Patterns

Crack patterns and deterioration of concrete along cracks were important indicators of damage. All specimens suffered major deterioration in the form of cracking and crushing of concrete in the beam plastic hinging zones, which included the sections of the main beams adjacent to the crossbeam with lengths along the beams approximately equal to overall beam depth. Many cracks formed in the beam stem and flange outside the hinging zones but, except for the cracks accompanying the final punching failure in the crossbeams of Specimens 1 and 2, the opening of cracks and degradation and crushing of concrete along cracks outside the hinging zones were not major contributors to specimen strength loss during cyclic loading.

The pattern of cracks which developed during the first cycle of loading of Specimen 2, shown in Fig. 3.9, may be considered typical for all specimens tested. During the first half-cycle of loading, flexural and flexure-shear cracks formed at uniform intervals and at varying slopes along the beam. A vertical crack formed at the face of the crossbeam in all specimens. During the second half-cycle of loading, cracks extended from the bottom face of the beam stem and intersected the cracks formed previously.

Cracks which formed during the first cycle of loading constituted the majority of all cracks which formed during the life of each specimen. During the second and subsequent cycles of loading, these cracks opened and closed as the member was deformed. Few new cracks formed. When large deformations were applied to the specimens (after Cycle 9), crushing and spalling of concrete occurred primarily in the beam hinging zones. Fig. 3.10 illustrates the nature of deterioration which had taken place in Specimen 2 by the fourth load cycle and at failure.

Crack patterns in the flanges of the specimens were indicative of the ability of shear reinforcement to confine the beam and flange laterally. Fig. 3.11(a) illustrates the cracks which occurred in the flange of Specimen 2. Crack patterns which developed in Specimen 1 were essentially identical to those shown in this figure. The majority of cracks formed at right angles to the beam axis. Longitudinal cracks, indicative of flange and beam lateral expansion, were small and few in number.

Cracking in the flange of Specimen 3, shown in Fig. 3.11(b), was much more severe than in either of the other two specimens. Longitudinal cracking was extensive, particularly in the plastic hinging regions. It is clear that the reinforcement used in Specimen 3 did not provide lateral confinement as effectively as that used in Specimens 1 and 2.

3.7 Failure Modes

The failure modes of the three specimens are discussed in this section. Specimens 1 and 2 suffered compression shear failures near the center crossbeam section during the 14th and 13th load cycles respectively. Each failed during the negative displacement portion of the load cycle.

The appearance of Specimens 1 and 2 at failure are shown in Figs. 3.12 and 3.13. Both failures consisted of the "punching through" of the center load ram attachment fixture, crushing of the concrete flange near the center crossbeam, and the separation of the flange from the web section of the center crossbeam. At failure, the cores of the beams of Specimen 1 were well segmented and crushed in the zones of inelastic hinging, as shown in Fig. 3.12(a). The cores of the longitudinal beams in Specimen 2 were not severely segmented or crushed at failure.

The appearance of both Specimens 1 and 2 at the conclusion of testing are shown in Fig. 3.13. Note that in Fig. 3.13(a) crushed concrete has been removed from the hinging zone immediately left of the crossbeam. Also note that the top longitudinal reinforcement of Specimen 1 was severely bent at failure. This appeared to result from the punching failure of the specimen and the large resulting local deformation rather than from buckling of the longitudinal bars.

Specimen 3 failed during the positive load portion of the 10th load cycle as a result of shear deterioration and loss of anchorage of stirrups in the portion of the beam west of the ram attachment point. Failure appeared to have been initiated by loss of anchorage of the stirrup hooks in the beam flange. The failure also comprised deterioration of the beam core just west of the center crossbeam and loss of lateral and vertical confinement of the beam flange. The appearance of Specimen 3 at failure is shown in Fig. 3.14.

3.8 Discussion of Observed Behavior

Previous sections of this report have presented examples of the types of measurements which were performed during the test of each specimen in

this investigation. Because the objective of the investigation was to determine the effect of stirrup-tie shape on behavior of the members tested, the collected data will be discussed in this section with that objective in mind.

(a) Load-Displacement Curves, Energy Dissipation

Energy dissipation measured for a particular member and the load vs. displacement curve for that member may best be considered together, as the two are interdependent and collectively provide a qualitative and quantitative measure of member performance.

An overall view of individual member behavior and differences in behavior among the three members tested may be obtained by examining the member load vs. displacement curves (Fig. 3.1). It must be noted that, although it had been intended that displacement history be uniform for the three specimens, actual displacement history for each specimen was unique due to differences in measurement of displacement at the point of loading and to difficulties in controlling load ram position.

If the displacement history of Specimen 2 is taken as a standard, the displacement histories used for the other specimens contain two major deviations from that standard. First, the displacement applied to Specimen 1 was based on displacement measured by an LVDT contained in the load ram. Displacements measured in this way ignored specimen support motion and elastic deformation of the load ram and the frame which supported the load ram. The load-displacement curve for Specimen 1 (Fig. 3.1a) has been corrected to eliminate these effects. During the tests of Specimens 2 and 3, an independent LVDT and measuring frame were used to obtain actual member deformations, which were in turn used as a basis for load application.

Second, a very large positive displacement was applied during the first cycle of loading of Specimen 3 as a result of failure of the ram control circuit. This was a one-time occurrence during which time the load ram moved continuously between a point of small displacement and the maximum first cycle displacement. This prevented the reading of the strain gages and LVDT's except at the two load points bounding this large excursion. Reading of load and displacement was not affected, as those values were plotted continuously as loading progressed.

The effect of these differences in displacement history can be determined by examining the energy dissipation values listed in Table 3.1. Again using the behavior of Specimen 2 as a standard, it is evident that Specimen 1 dissipated a smaller amount of energy per cycle than did Specimen 2. The major part of this difference must be attributed to the difference in displacement history between the two specimens. Because Specimen 1 dissipated a larger amount of energy than did Specimen 2 prior to failure, it is reasonable to speculate that Specimens 1 and 2 would have dissipated essentially identical amounts of energy during the first eight load cycles if their displacement histories had been identical.

Similar speculation is possible with regard to the probable energy dissipation capacity of Specimen 3 during a displacement history similar to that experienced by Specimen 2. It is clear that Specimen 3 dissipated much more energy than did Specimen 2 during the first eight cycles of load as a result of their differing displacements during load cycle 1. It is not clear exactly how their capacities would have compared under identical load histories. Two factors must be considered. First, the amount of energy dissipated by Specimen 3 during the first load cycle would have

been greatly reduced by limiting positive displacement to 0.75 in. (19 mm) during that load cycle. Second, it is possible that Specimen 3 would have dissipated slightly more energy and would have endured more cycles of load if it had not been softened and extensively cracked by its initial large deflection. It is important to note that all three specimens tested dissipated comparable amounts of energy during load cycles 2-8. It is logical to predict that all three would have performed comparably during load cycles 1-8 if they had been deflected comparably.

(b) Relationship of Steel Strains to Load and Displacement

The relationships between various steel strains and load and displacement, shown in Fig. 3.2 through 3.6, are remarkable primarily in that the relationships remain essentially uniform for all specimens tested. This is particularly true for the first eight cycles of loading, the portion of the displacement history which had been intended to simulate the total demands which might arise from severe earthquake loading.

The uniformity of the relationship of strain in top longitudinal reinforcement to load for the three specimens can be seen in Fig. 3.2. In Figs. 3.2(a) and 3.2(b), the load point at which steel yield was suggested by specimen load-deflection behavior is indicated as point A. Because this point occurs at the bar yield strain, the behavior of the material is confirmed by behavior of the specimen. In the case of Specimen 3, loading could not be stopped when steel yield was suspected. An estimated relationship of load to steel strain during Load Cycle 1 has been shown as a dashed line in the plot for Specimen 3, Fig. 3.2(c).

The gradual increase in tensile strain of both top and bottom longitudinal steel during cyclic loading, evident in Figs. 3.2 and 3.3, is a

characteristic of steel strain conditions in members subject to repeated inelastic flexure. It has been speculated that this behavior is caused by the inability of cracks to close completely after having been opened by plastic hinging deformations because of small amounts of offset along the crack and because small chips of concrete may lodge in the cracks as the member deteriorates. This causes the member to increase in length during cyclic loading, a behavior that had been anticipated and one which was seen in these tests, as each member increased in length by slightly over 1 in. (25 mm) during loading.

The relationship of load point displacement to strain in the vertical legs of two stirrups of each specimen is shown in Figs. 3.4 and 3.5. The magnitudes of measured strains in each stirrup during any given cycle of load were comparable for all specimens. It is interesting to note that yield strains were developed during the eighth cycle of loading in the stirrup to which gage 2 had been attached in Specimen 3. This indicates that anchorage of those stirrup legs was still acceptable at that time.

The character of the relationships of beam load point displacement to flange transverse strain as measured by gage 3 has been considered previously. The most important point to note here is that the magnitude of strains measured by this gage was comparable for all specimens during the first eight cycles of loading. During the tenth and succeeding cycles of loading the lateral strains measured in Specimen 3 were larger than those measured in the other specimens, indicating that lateral confinement provided by the flange for the top portion of Specimen 3 was decreasing. This was visually confirmed by the large amounts of longitudinal cracking which took place in Specimen 3. The other two specimens suffered neither this degree of loss of confinement nor such extensive longitudinal cracking.

(c) Failure Modes

The failure modes of Specimen 1 and 2 cannot be related to stirrup-tie shape. It is doubtful that the punch-through of the center load ram support could have been prevented by any practical changes in beam shear reinforcement. Because the final failures of Specimens 1 and 2 occurred only after very large displacements (6% of shear span) had been imposed, and because the test apparatus produced symmetric bending at the point of load application as opposed to the unsymmetric bending that would take place in an actual structure during earthquake loading, the failure modes of Specimens 1 and 2 almost certainly would not occur in an actual structure.

The failure mode of Specimen 3 was directly attributable to stirrup-tie shape, as had been the intent during design. Although this design is not proposed for use, it performed much better than had been anticipated. As strain gage readings indicated, the lateral flange strain in Specimen 3 was not appreciably greater than that in the other two specimens. This indicates that the floor slab (beam flange) provided much better lateral confinement to the beam core during inelastic cyclic loading than had been predicted previously.

It should also be noted that longitudinal beam steel in Specimen 3 was arranged so that no bar was located at the inside of the stirrup legs top bends. While it may be presumed that member behavior would have been improved if ACI code recommendations in this regard had been followed, it is impossible to predict accurately how much improvement would have resulted.

CHAPTER 4

SUMMARY AND CONCLUSIONS

4.1 Summary of Research

The objective of the research was to determine the influence of stirrup-tie shape on the behavior of reinforced concrete flanged members (T-beams) subjected to repeated reversed inelastic flexure. Three double cantilever flanged beams were subjected to static cyclic load. The only test variable was the shape of the stirrups or ties used as beam shear reinforcement.

A single style of stirrup or tie was used in the zones of inelastic flexure in each of the three specimens. The types of ties used were: (1) closed hoops conforming to the requirements of Appendix A of the American Concrete Institute Building Code (Ref. 1), (2) U-shaped stirrups in which the tops of the vertical legs terminated in 180 degree standard hooks, and (3) U-shaped stirrups in which the tops of the vertical legs terminated in 90 degree hooks bent outward, or away from the beam core. The spacing of shear reinforcement was the same for all members, and longitudinal steel proportions and locations were the same for all members.

Specimens were supported near their ends by pins intended to simulate simple supports and vertical loads were applied to the center of the specimen by a double-acting hydraulic ram. Static cyclic loads were applied to produce deflections of the center of the specimens of between 0.75 in. and 3 in. (19 and 76 mm), or 1.5 percent and 6 percent of the beam shear spans. Maximum deflection during the first eight cycles of loading was three percent of beam shear span (1.5 in., 38 mm).

Evaluation of specimen behavior was based on visual observations of concrete cracking and deterioration, load vs. displacement relationships, and measurements of steel strains and beam flexural rotations.

4.2 Summary of Observed Behavior

(1) The specimens having shear reinforcement consisting of closed hoops or stirrups with 180 degree hooks (Specimens 1 and 2) endured large displacements without severe strength or stiffness decay. Final failure of these specimens consisted of a punching failure of the specimen flange in the region of the point of load ram attachment. It was concluded that this type of failure would be very unlikely in an actual structure during an earthquake because of the inherently different loading conditions and support conditions which would exist in a real structure as opposed to those present in the test situation.

(2) The specimen whose shear reinforcement consisted of stirrups with 90 degree hooks bent away from the beam core (Specimen 3) failed as a result of loss of anchorage of stirrups which terminated in the flange of the specimen. It was concluded that this type of failure could occur in a real structure under deflection conditions similar to those experienced by the test specimen.

(3) Lateral strains in the flange of the specimens as measured by strain gages placed on the stirrups and on lateral temperature steel were comparable for all specimens.

(4) All specimens were able to endure eight cycles of inelastic flexure with maximum displacements of between 1.5 percent and 3.0 percent of beam shear span. All specimens dissipated approximately equal amounts of energy during the second through eighth load cycles. Overall specimen behavior indicated that approximately equal amounts of energy would have

been dissipated by the specimens during the first eight load cycles if identical displacement histories had been used for all specimens during those load cycles.

4.3 Conclusions

On the basis of the test results previously discussed, the following conclusions can be drawn:

(1) There was no significant difference in cyclic behavior between the specimens containing closed-hoop shear reinforcement (Specimen 1) and the specimen containing shear reinforcement consisting of U-shaped stirrups with vertical legs terminating in 180 degree hooks (Specimen 2).

(2) The flange of the beams provided a significant amount of lateral confinement to the upper portion of the beam core in the region of plastic hinging.

(3) There is reason to believe that, for flanged sections or beams cast monolithically with slabs, present recommendations requiring closed hoops as shear reinforcement may be too conservative and may cause difficulty in construction which could be avoided by using U-shaped stirrups with 180 degree standard hooks.

4.4 Recommendations for Future Research

The influence of stirrup-tie shape on cyclic inelastic response of reinforced concrete flexural members has been considered only briefly in this investigation. The following topics are logical extensions of the work begun here:

(1) The behavior of a beam similar in proportion to Specimen 3 but having a longitudinal bar located inside the bends of the stirrup leg hooks should be considered.

(2) The behavior of beams with a flange on only one side of the beam stems (spandrel beams) and having various tie shapes should be considered.

(3) Work should be done to consider the effect of lateral compressive stiffness of the beam flange on confinement of the beam core. This could be done by providing lateral reinforcement larger than that required for temperature and shrinkage to more accurately simulate the magnitude of lateral flange compressive stiffness which would be present in an actual structure.

SELECTED REFERENCES

1. ACI Committee 318, "Building Code Requirements for Reinforced Concrete (ACI 318-77)," American Concrete Institute, Detroit, 1977, 102 pp.

2. Ma, S.Y.M., Bertero, V.V., and Popov, E.P., "Experimental and Analytical Studies on the Hysteretic Behavior of Reinforced Concrete Rectangular and T-Beams," Earthquake Engineering Research Center, Report No. EERC-76/2, University of California, Berkeley, 1976.

3. Behera, U. and Rajagopalan, K.S., "Two-Piece U-Stirrups in Reinforced Concrete Beams," ACI Journal, Proceedings, V. 66, No. 7, July 1969, pp. 522-524.

4. Gosain, N.K., Brown, R.H., and Jirsa, J.O., "Shear Requirements for Load Reversals on RC Members," Journal of the Structural Division, ASCE, Vol. 103, No. ST7, Proc. Paper 13090, July 1977, pp. 1461-1476.

TABLE 2.1 Measured Dimensions of Specimens

Specimen No.	d, in (mm)	d', in (mm)	h, in (mm)	b, in (mm)	b_w, in (mm)	t_f, in (mm)	a, in (mm)	A_s, in^2 (mm^2)	A_s', in^2 (mm^2)	A_v, in^2 (mm^2)
1	11.6 (295)	2.6 (66)	14.0 (356)	32.0 (813)	8.0 (203)	4.1 (104)	50.0 (1270)	2.0 (1290)	2.0 (1290)	0.22 (142)
2	11.6 (295)	2.5 (64)	14.0 (356)	32.0 (813)	8.0 (203)	4.0 (102)	50.0 (1270)	2.0 (1290)	2.0 (1290)	0.22 (142)
3	11.6 (295)	2.4 (61)	14.0 (356)	32.0 (813)	8.0 (203)	4.1 (104)	50.0 (1270)	2.0 (1290)	2.0 (1290)	0.22 (142)

TABLE 2.2 Measured Concrete Strengths and Age at Testing

Specimen No.	Compressive Strength, psi (MPa)		Splitting Strength, psi (MPa)	Cylinder Age, days
	Batch 1	Batch 2		
1	3710 (25.6)	3740 (25.8)	257 (1.8)	48
2	4370 (30.1)	4310 (29.7)	363 (2.5)	44
3	4400 (30.3)	4330 (29.8)	350 (2.4)	45

TABLE 2.3 Measured Steel Properties

Bar Size	f_y,ksi (MPa)	f_u,ksi (MPa)	E_s,ksi (MPa)	E_{sh},ksi (MPa)	ε_{sh}	ε_u
#3	69 (475)	103 (710)	29,000 (200,000)	1120 (7720)	0.012	0.10
#4	71 (489)	110 (758)	30,000 (207,000)	1330 (9160)	0.0075	0.0098
#7	68 (468)	112 (772)	30,000 (207,000)	1440 (9920)	0.0039	0.096
#9	63 (434)	97 (668)	29,500 (203,000)	1210 (8340)	0.0066	0.097

TABLE 3.1 Measured Energy Dissipation

Load Cycle	Energy Dissipated, in-K (N-m) Specimen 1		Specimen 2		Specimen 3	
1	32.7	(3690)	50.8	(5740)	99.0	(11,180)
2	20.3	(2290)	33.8	(3820)	31.7	(3580)
3	22.3	(2520)	28.8	(3250)	24.9	(2810)
4	50.2	(5670)	55.0	(6210)	49.1	(5550)
5	39.8	(4500)	50.7	(5730)	49.4	(5580)
6	37.5	(4240)	44.6	(5040)	46.4	(5240)
7	110	(12,430)	112	(12,650)	108	(12,200)
8	112	(12,650)	107	(12,090)	108	(12,200)
9	18	(2030)	14.3	(1620)	13.1	(1480)
10	150	(16,950)	157	(17,740)	161	(18,190)
11	201	(22,710)	200	(22,600)		--
12	254	(28,700)	209	(23,610)		--
13	232	(26,210)	266	(30,050)		--
14	173	(19,550)		--		--
TOTAL, CYCLES 1-8	425	(47,990)	483	(54,530)	517	(58,340)
TOTAL	1450	(164,140)	1330	(150,150)	691	(78,010)

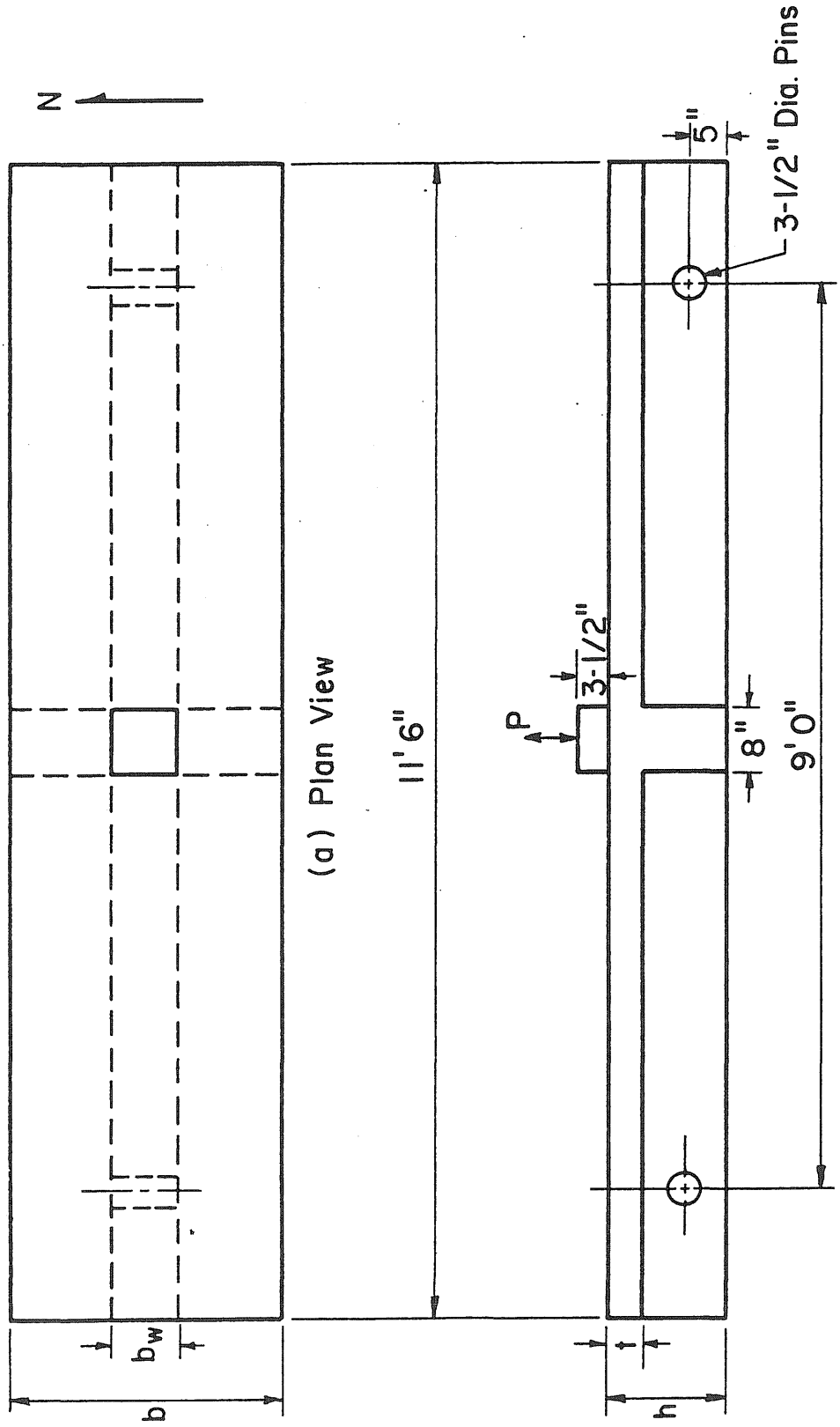

Note: 1 in. = 25.4 mm

Fig. 2.1 Plan and Side Views of Specimen

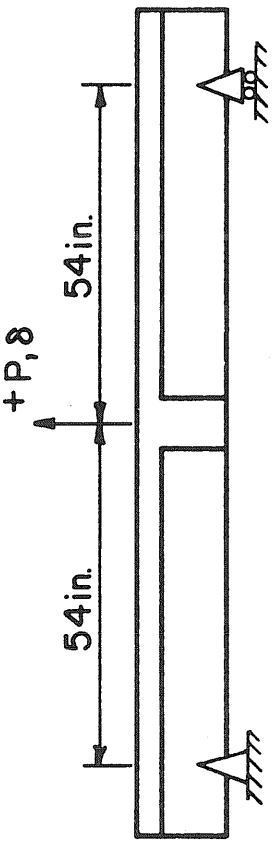

Fig. 2.2 Support Conditions and Load Application

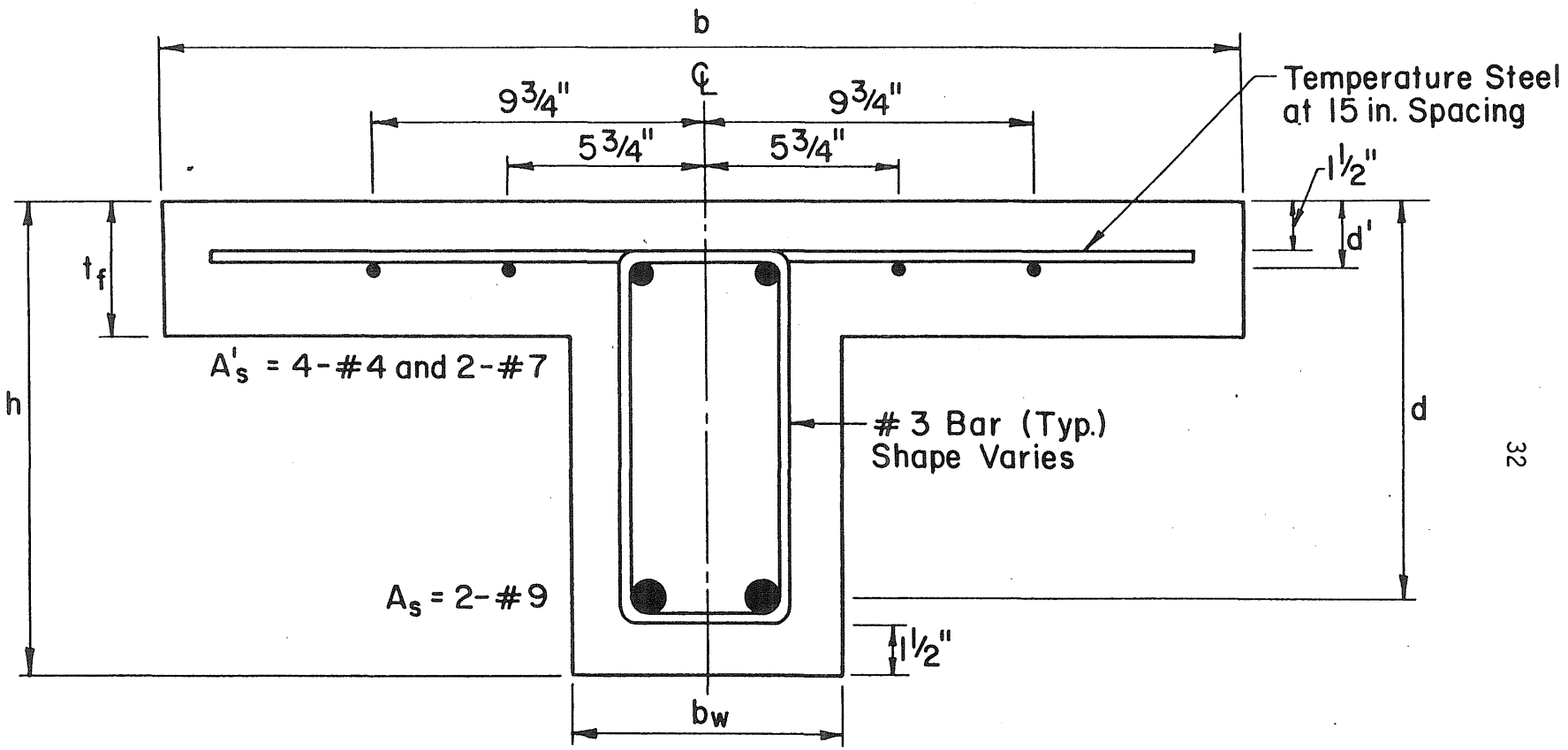

Fig. 2.3 Typical Cross Section of Specimen

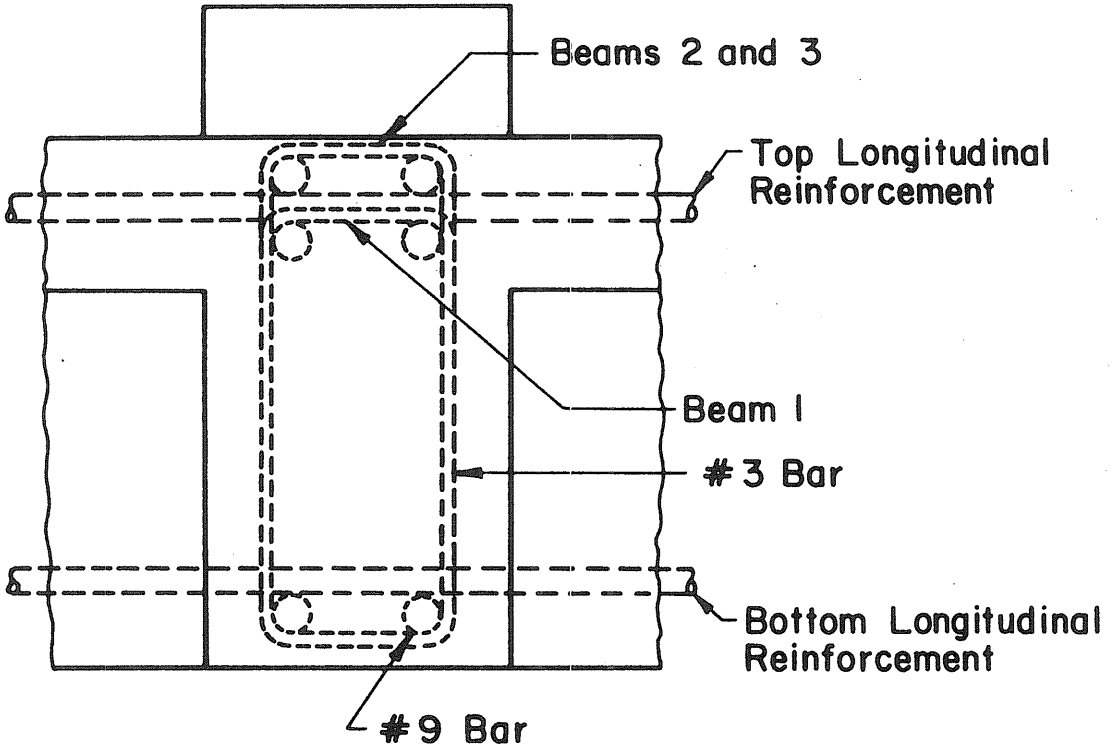

Fig. 2.4 Typical Cross Section of Crossbeam

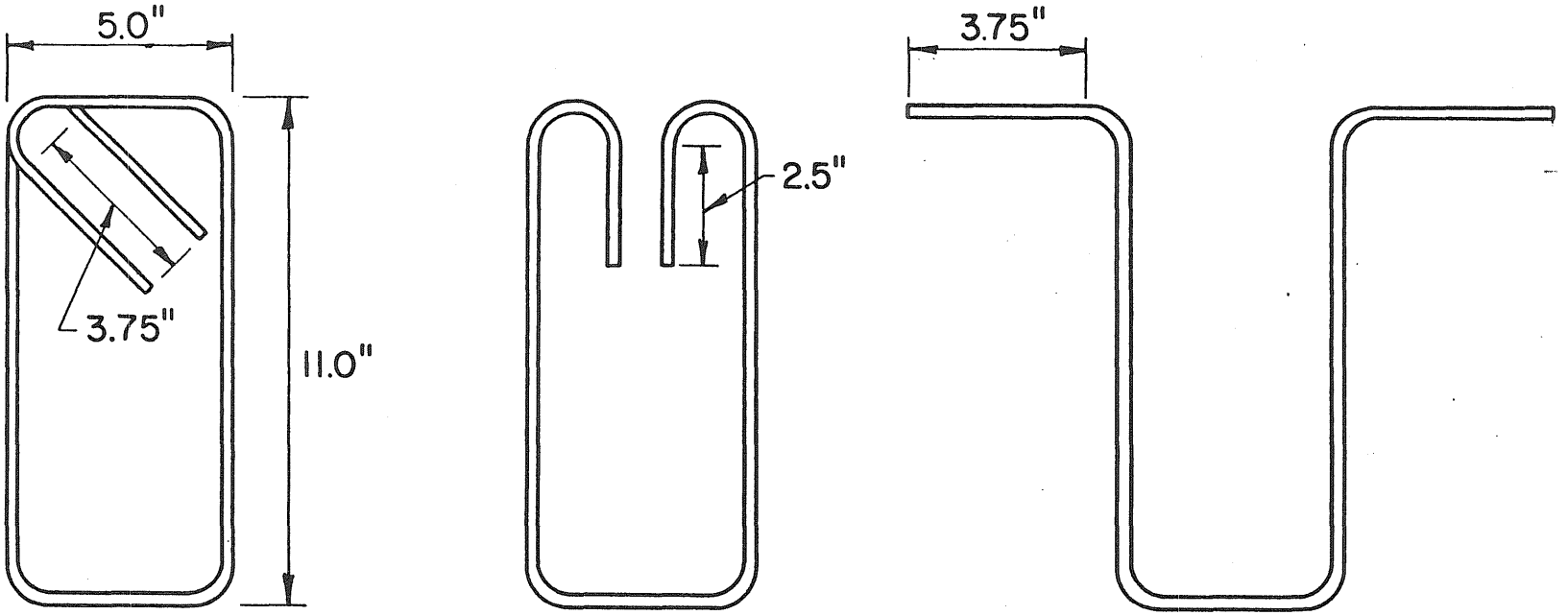

(a) Type I
(Beam 1)

(b) Type IV
(Beam 2)

(c) Type V
(Beam 3)

Fig. 2.5 Stirrup Configurations

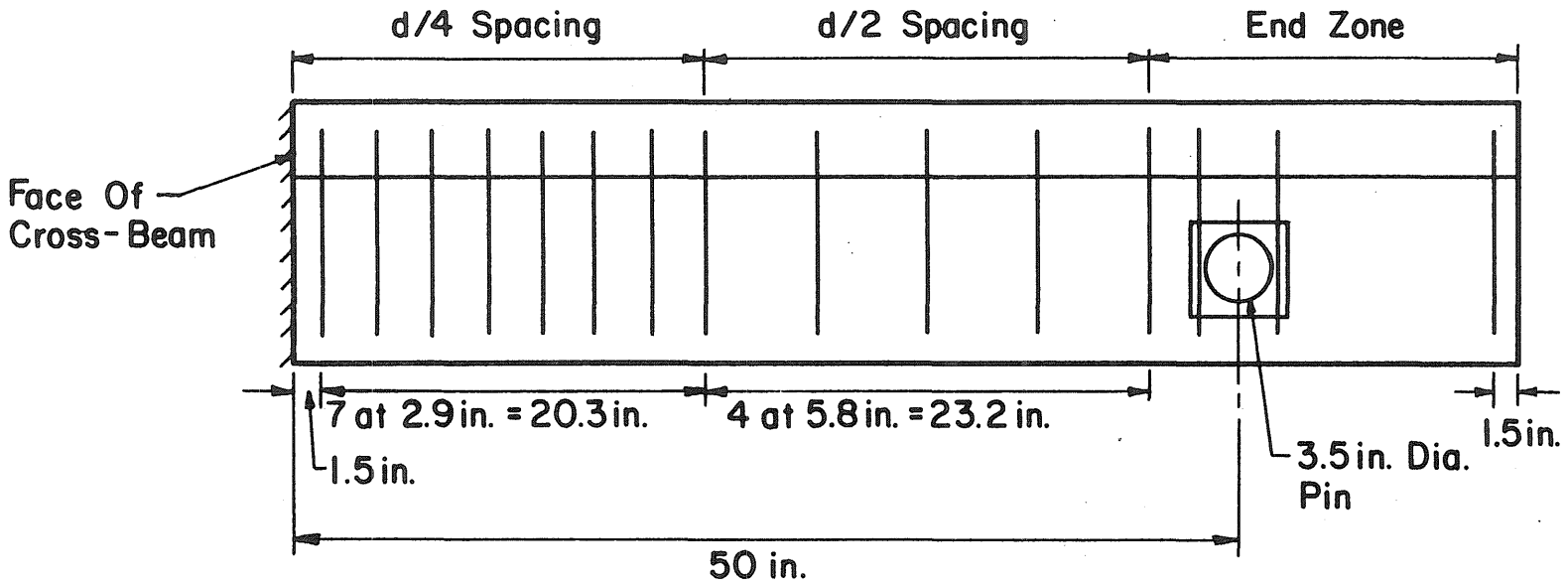

Fig. 2.6 Spacing of Shear Reinforcement

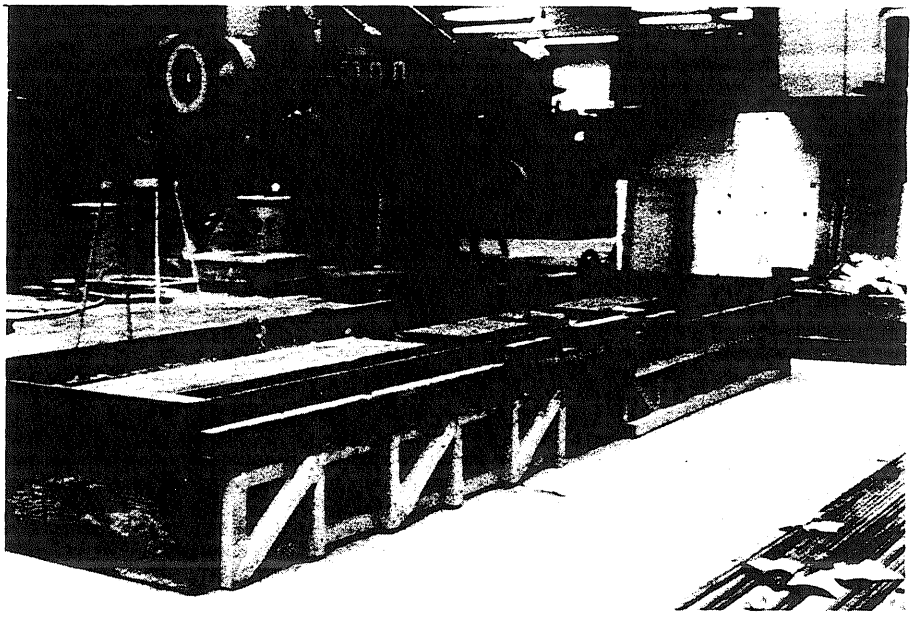

Fig. 2.7 Formwork in Position for Casting

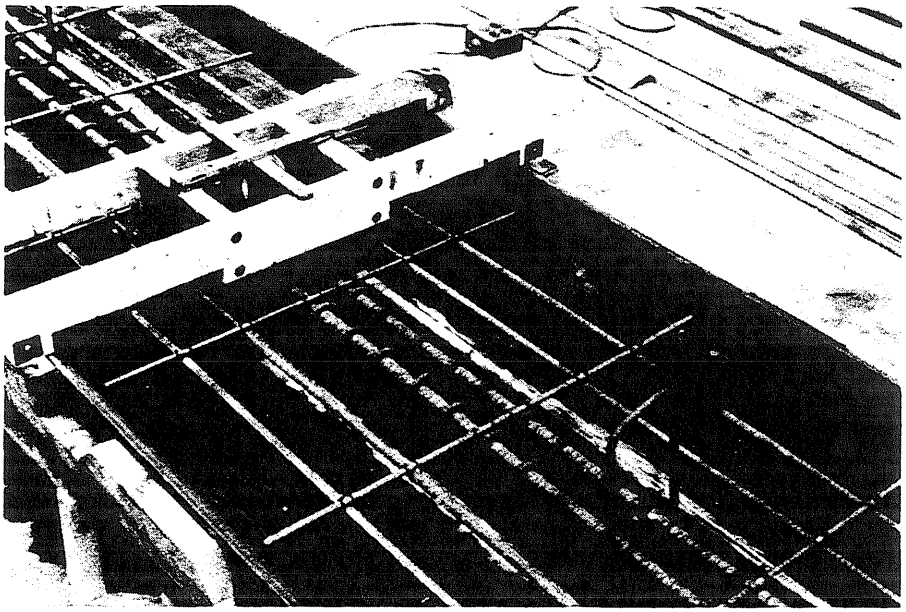

Fig. 2.8 Formwork with Reinforcement in Place

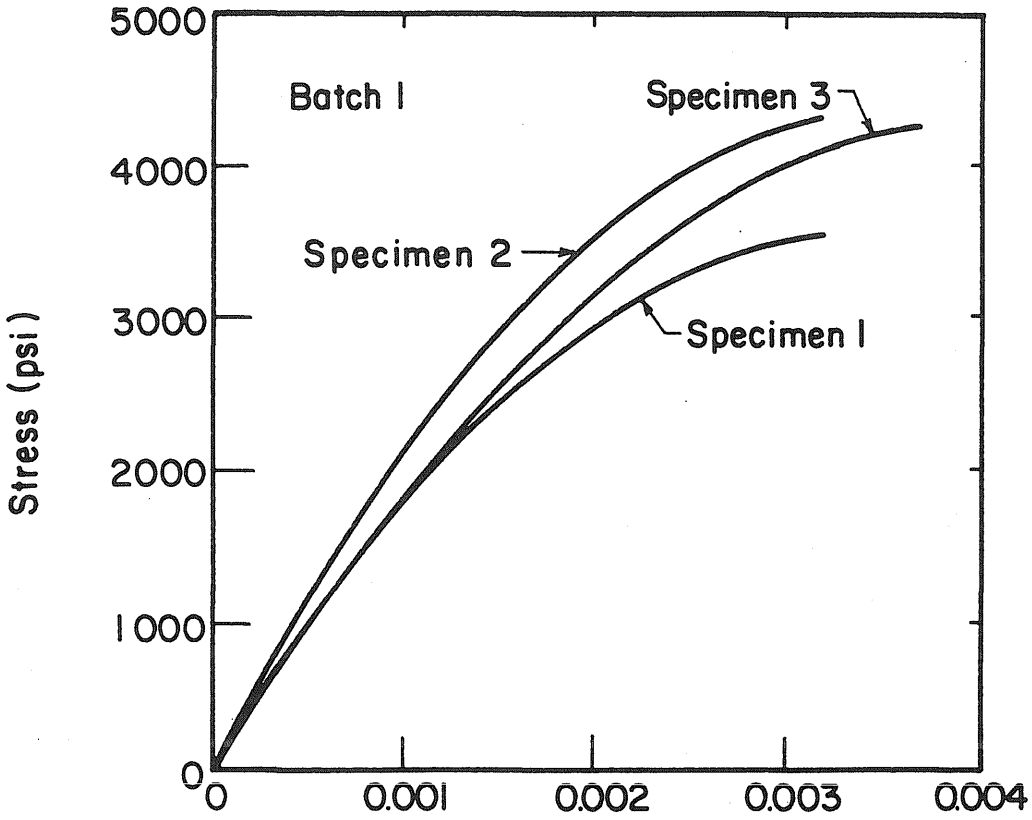

(a) Batch 1

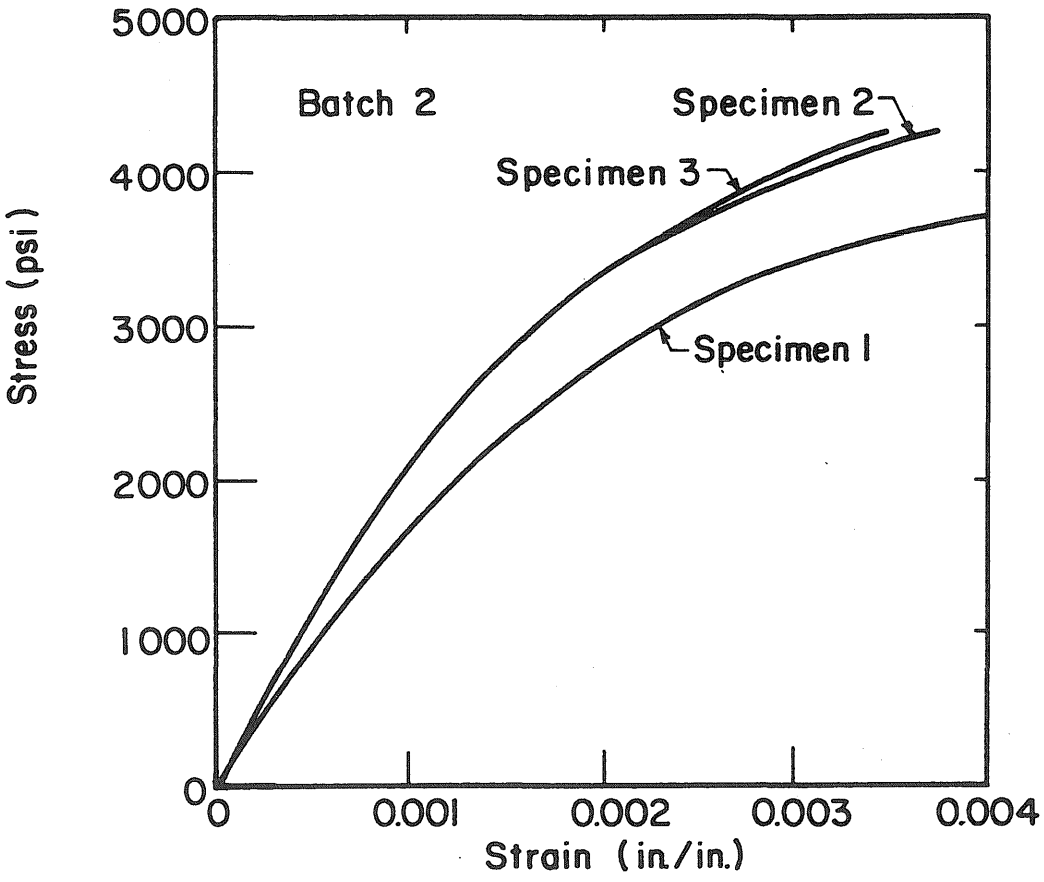

(b) Batch 2

Fig. 2.9 Concrete Stress-Strain Relationships

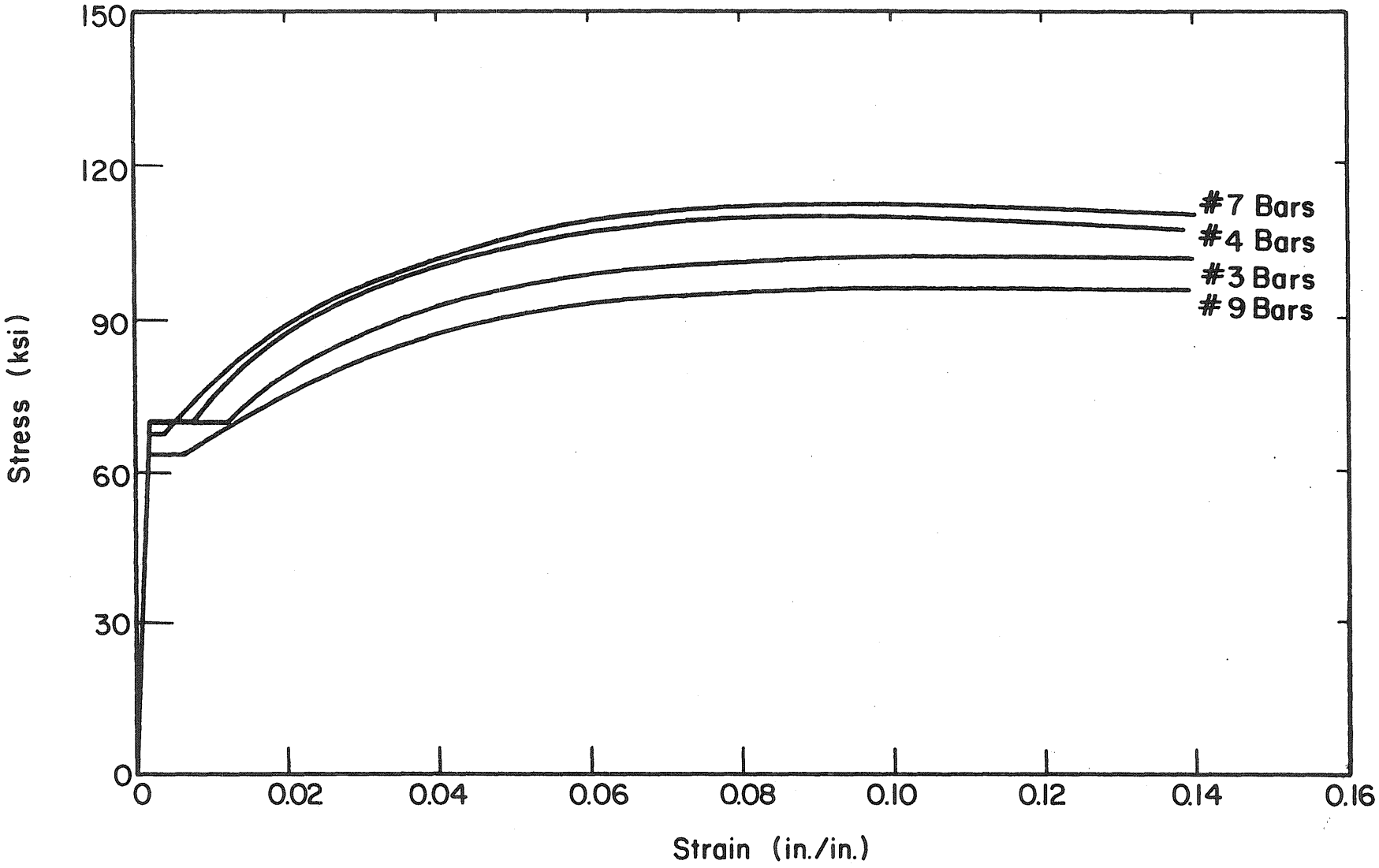

Fig. 2.10 Steel Stress-Strain Relationships

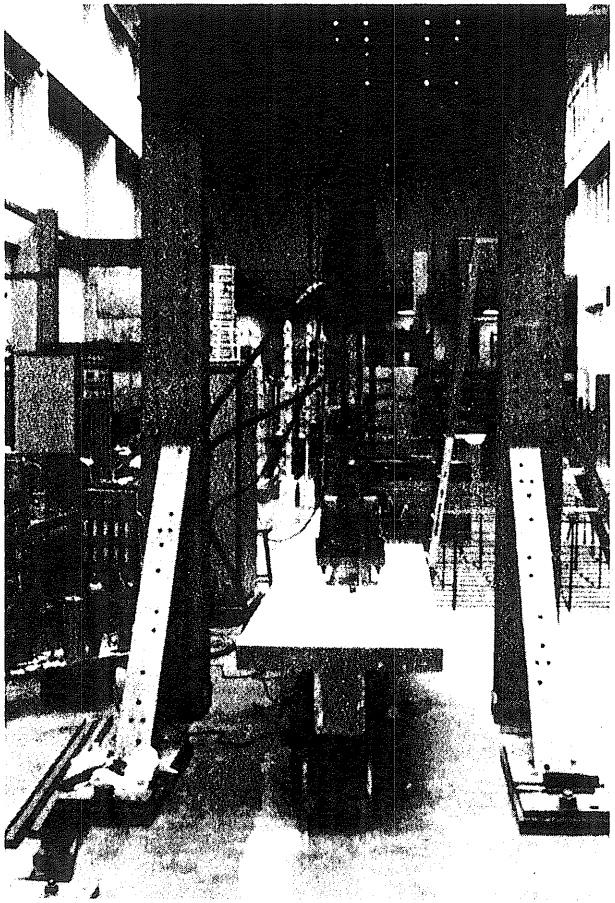

(a) Specimen 1

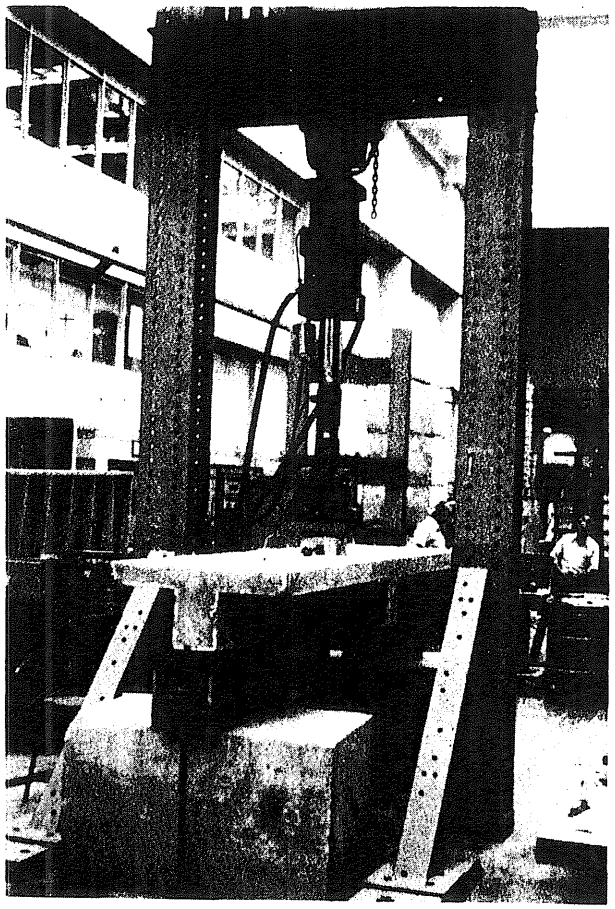

(b) Typical Setup for Specimens 2 and 3

Fig. 2.11 Specimens in Position on Supports Showing Load Ram and Frame

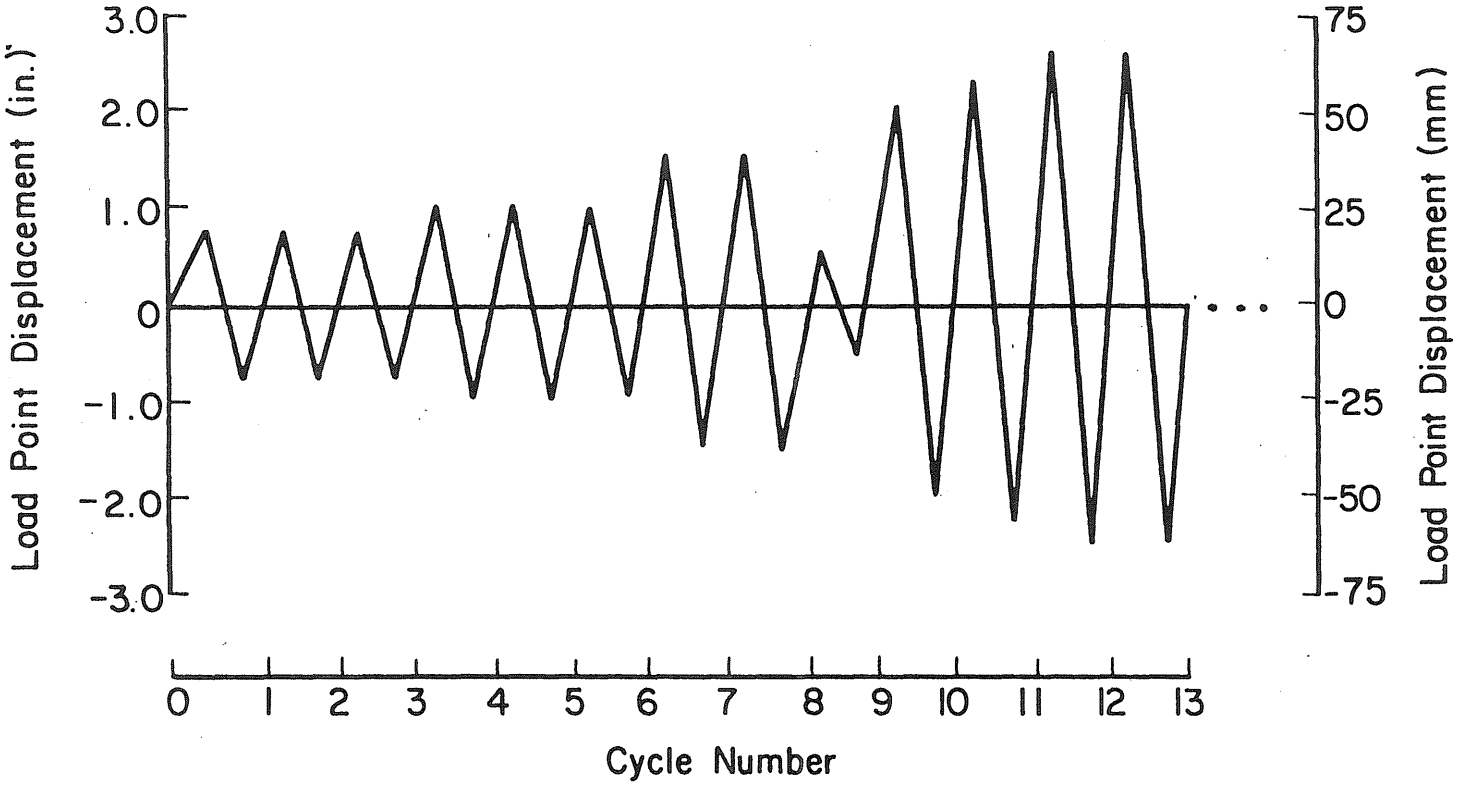

Fig. 2.12 Displacement Pattern

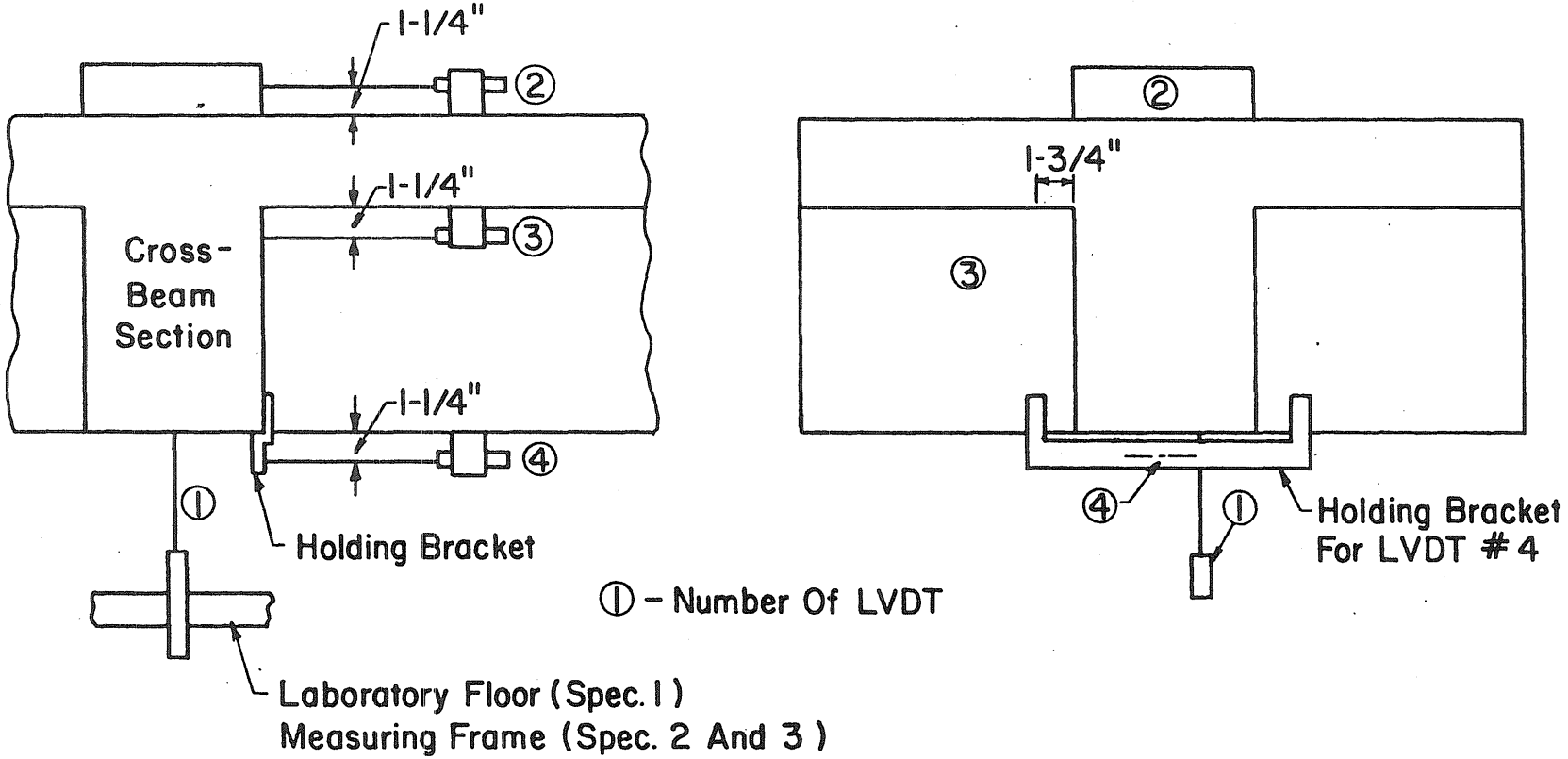

(a) View From North Side

(b) View From West Side

Fig. 2.13 LVDT Locations

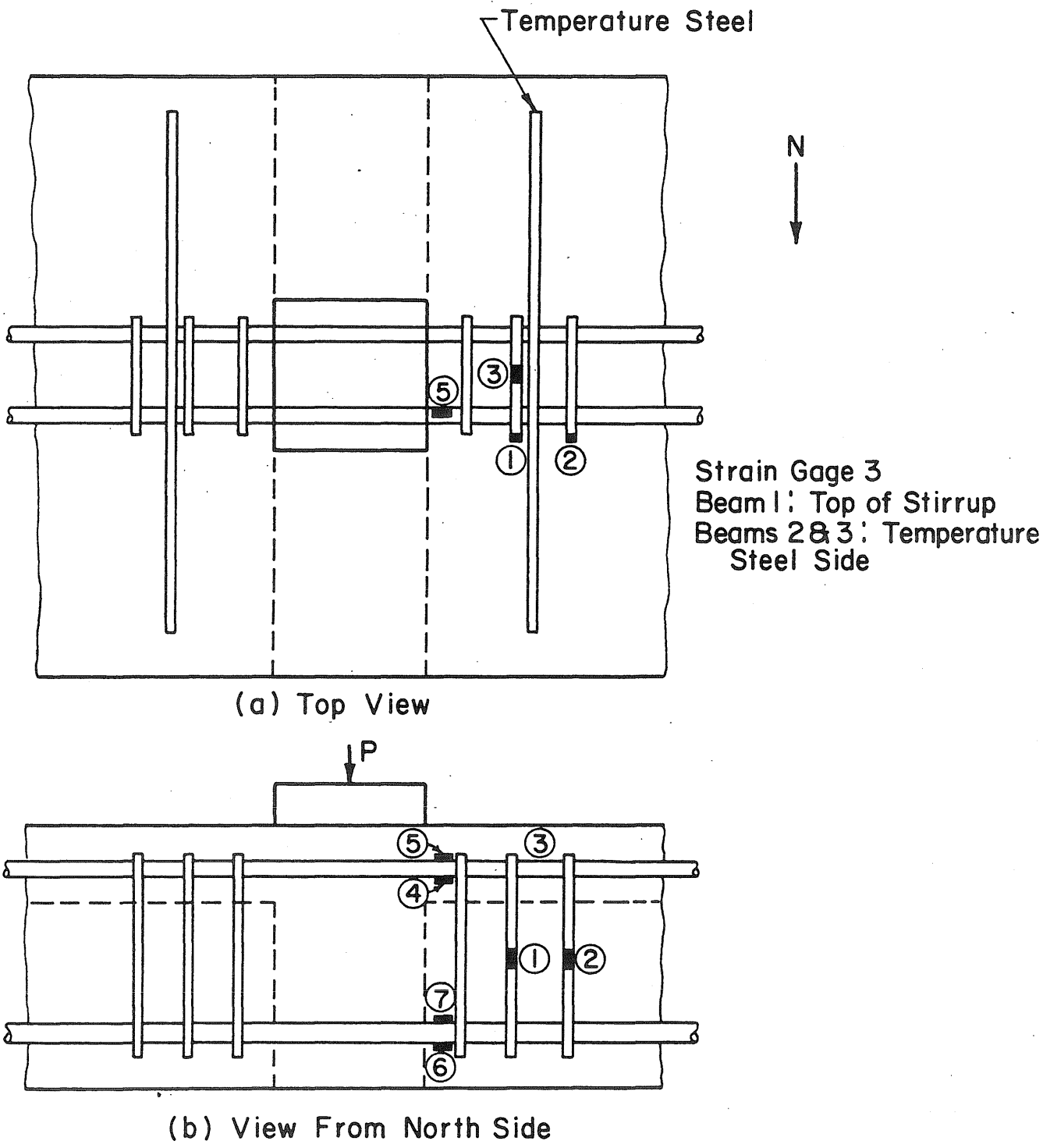

Fig. 2.14 Strain Gage Locations

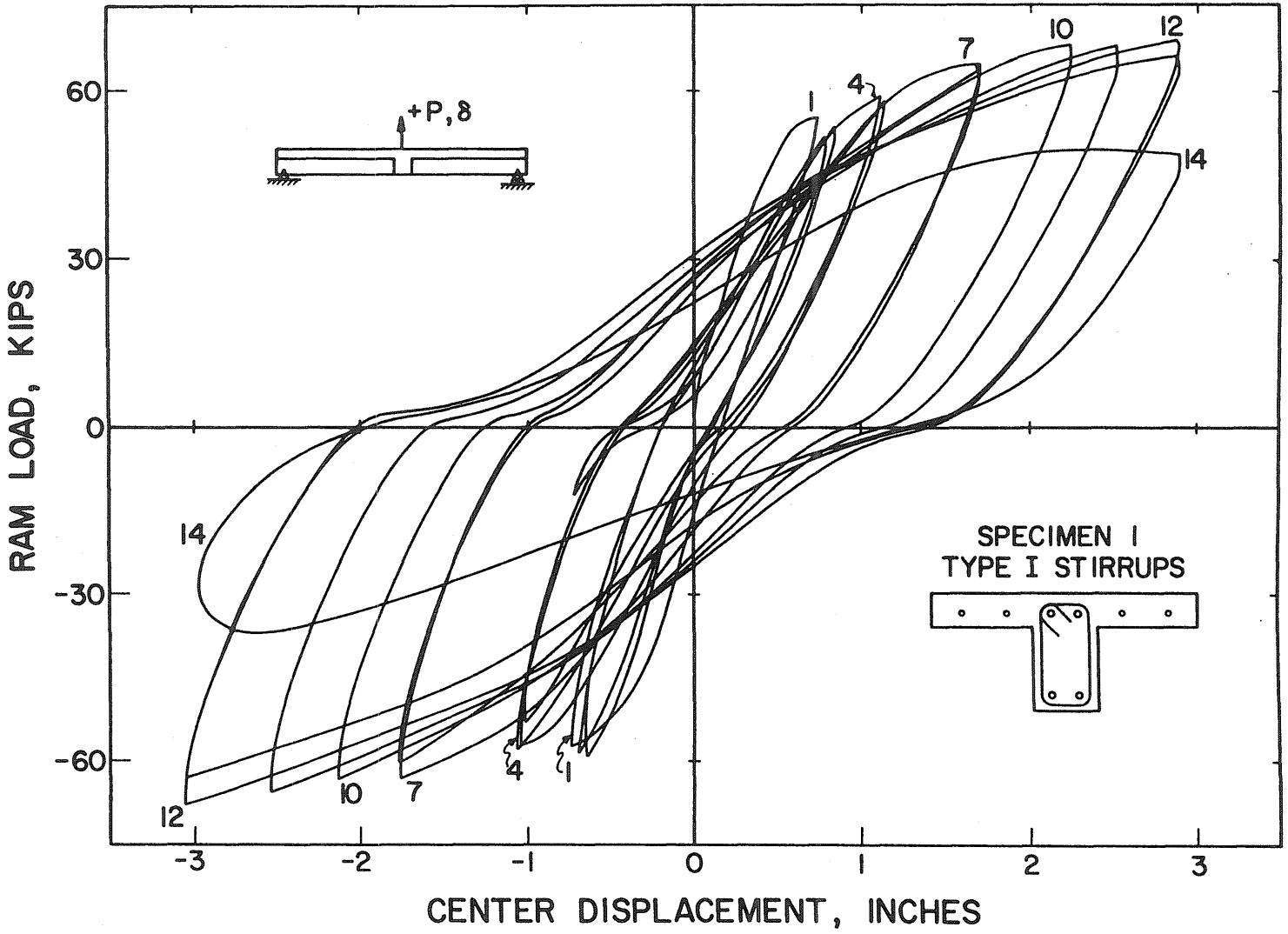

3.1a Load vs. Displacement Relationship--Specimen 1

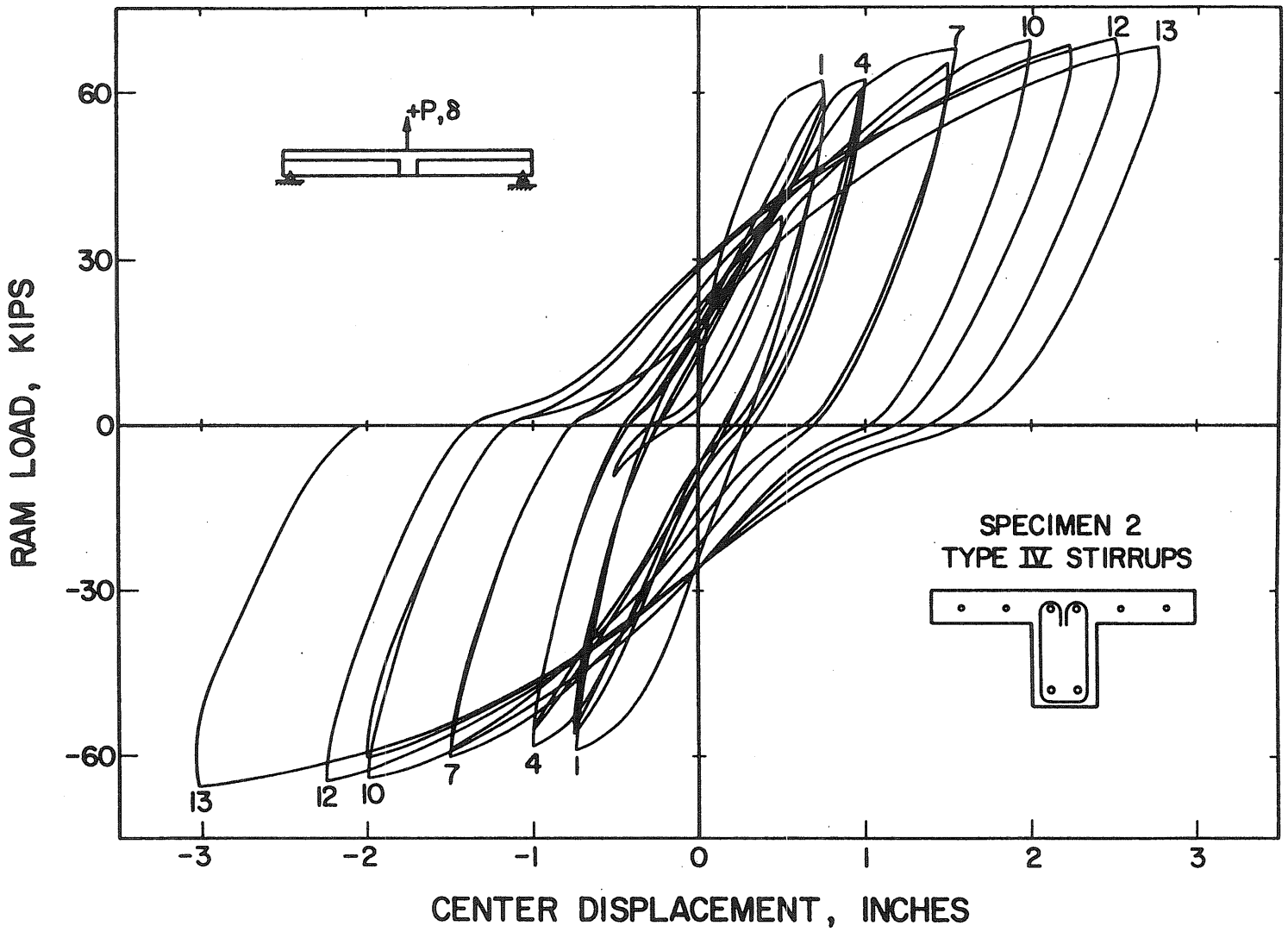

3.1b Load vs. Displacement Relationship--Specimen 2

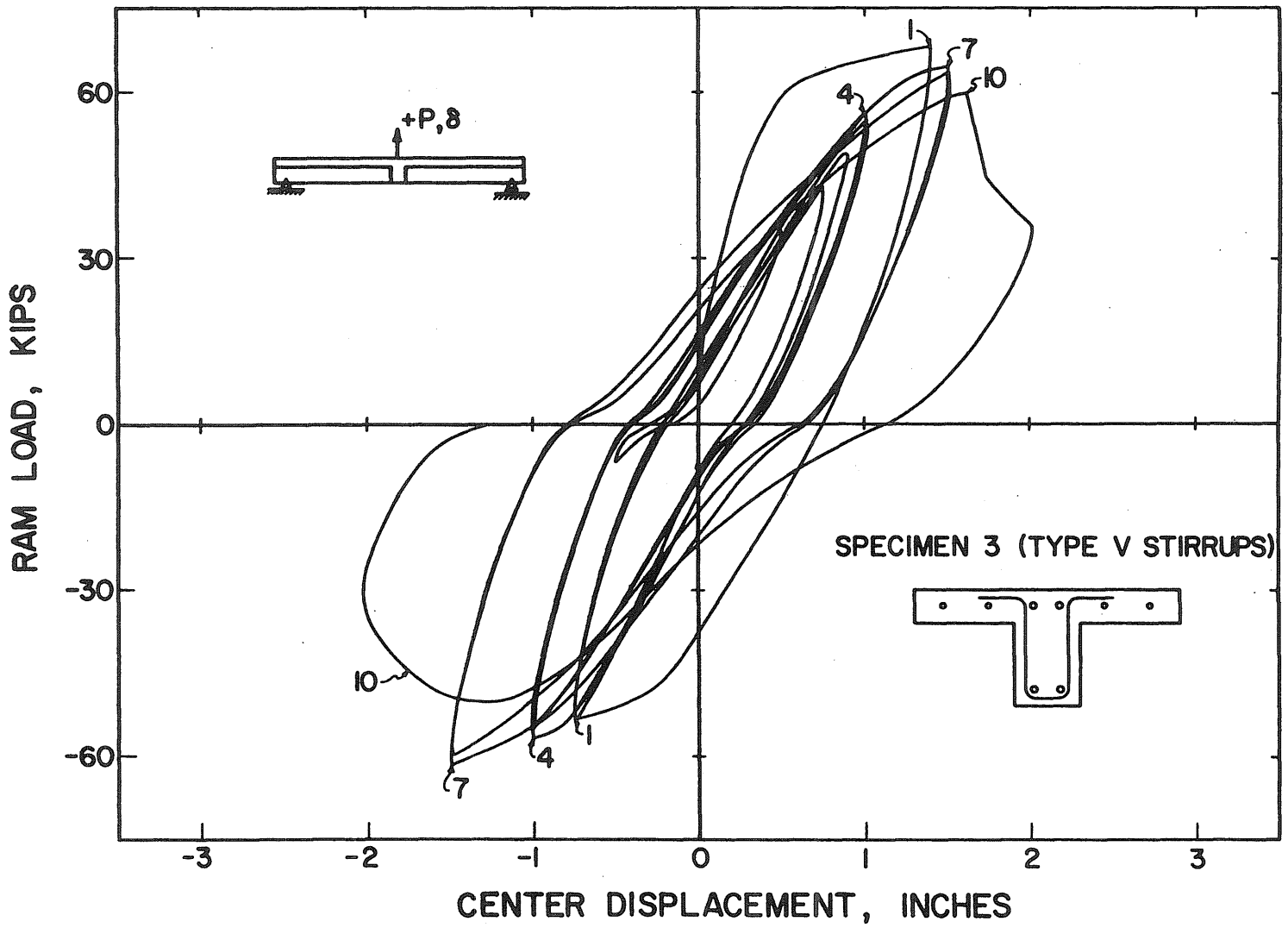

3.1c Load vs. Displacement Relationship--Specimen 3

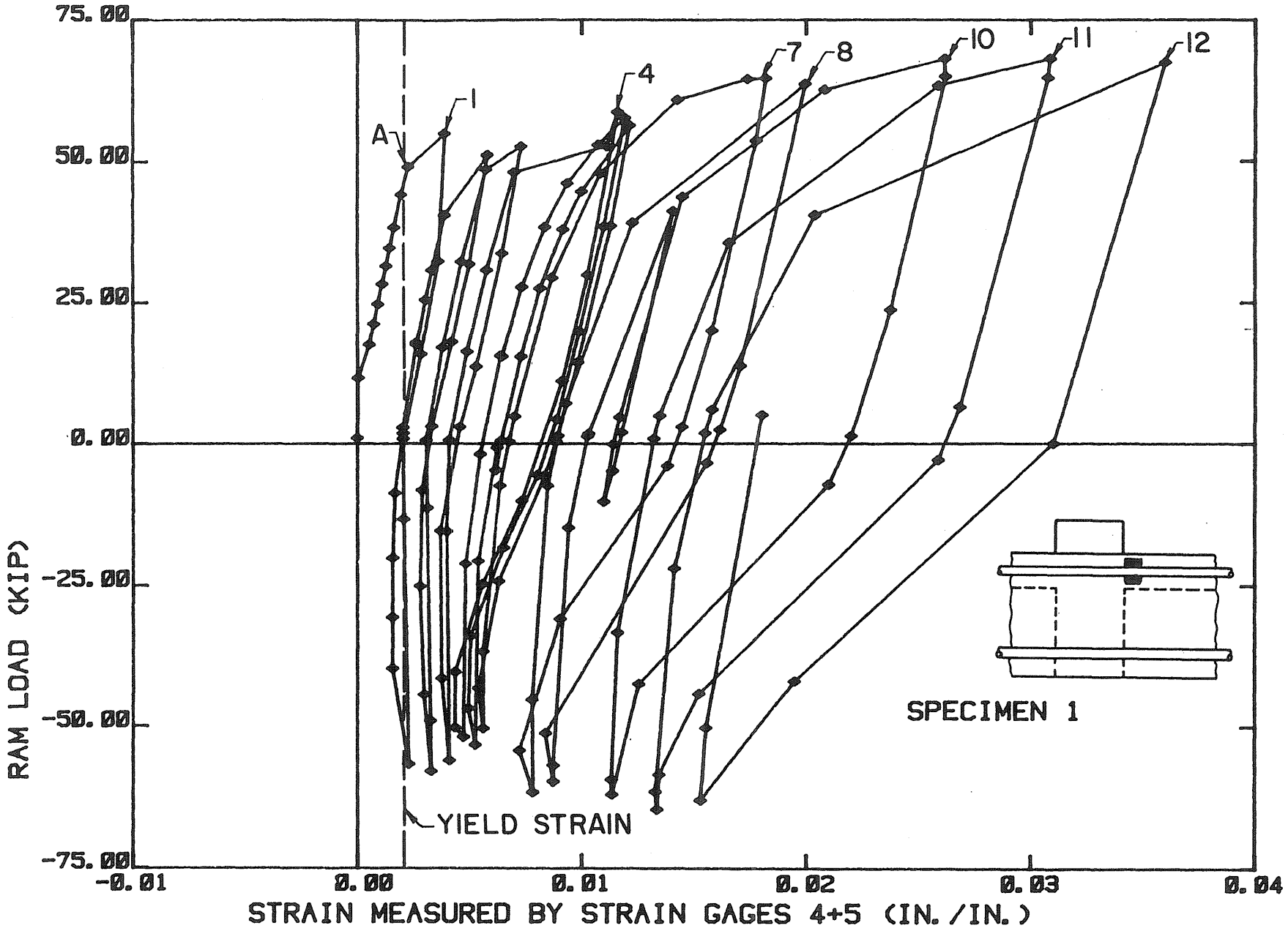

Fig. 3.2a Ram Load vs. Strain in Top Steel--Specimen 1

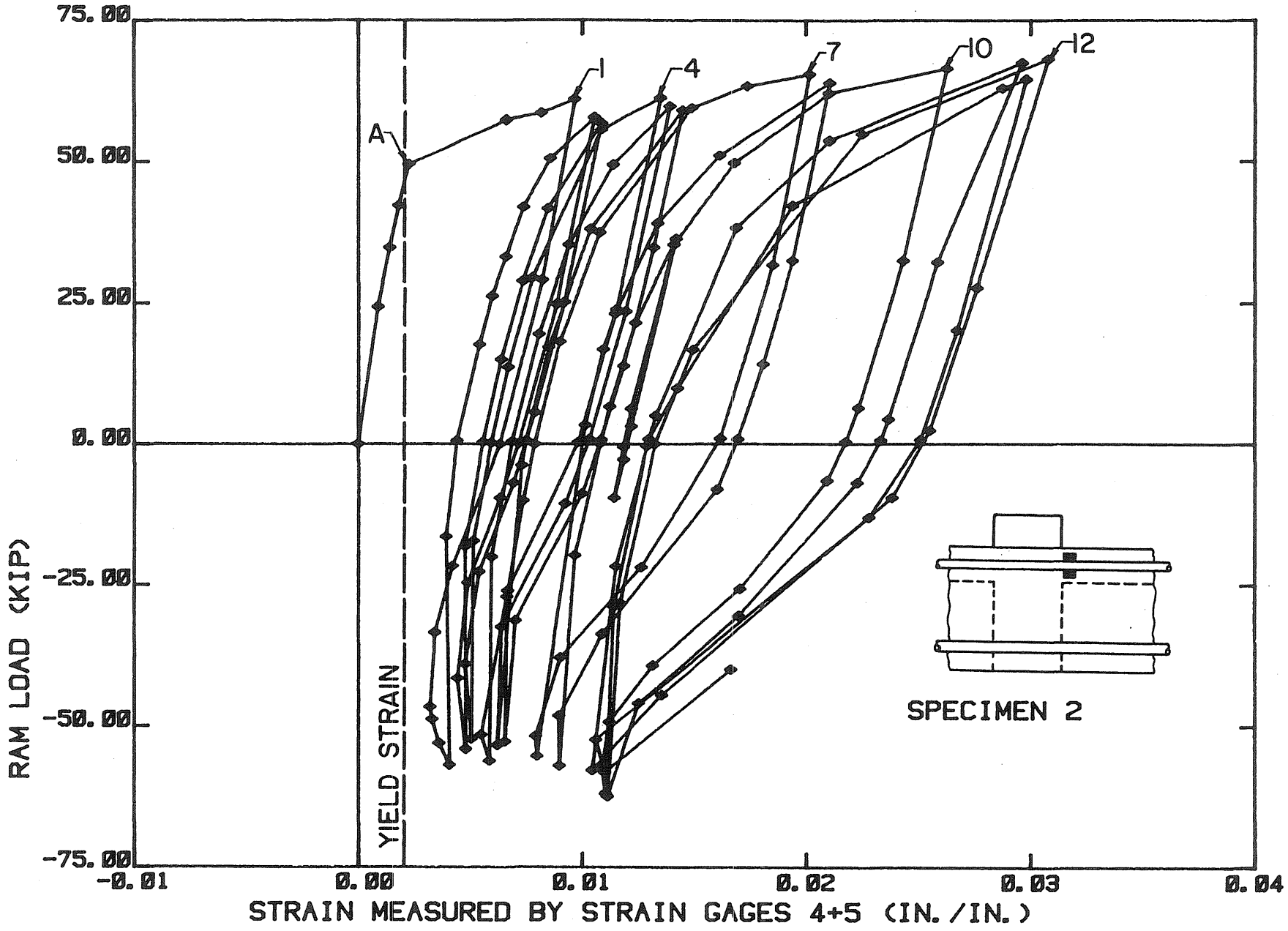

Fig. 3.2b Ram Load vs. Strain in Top Steel--Specimen 2

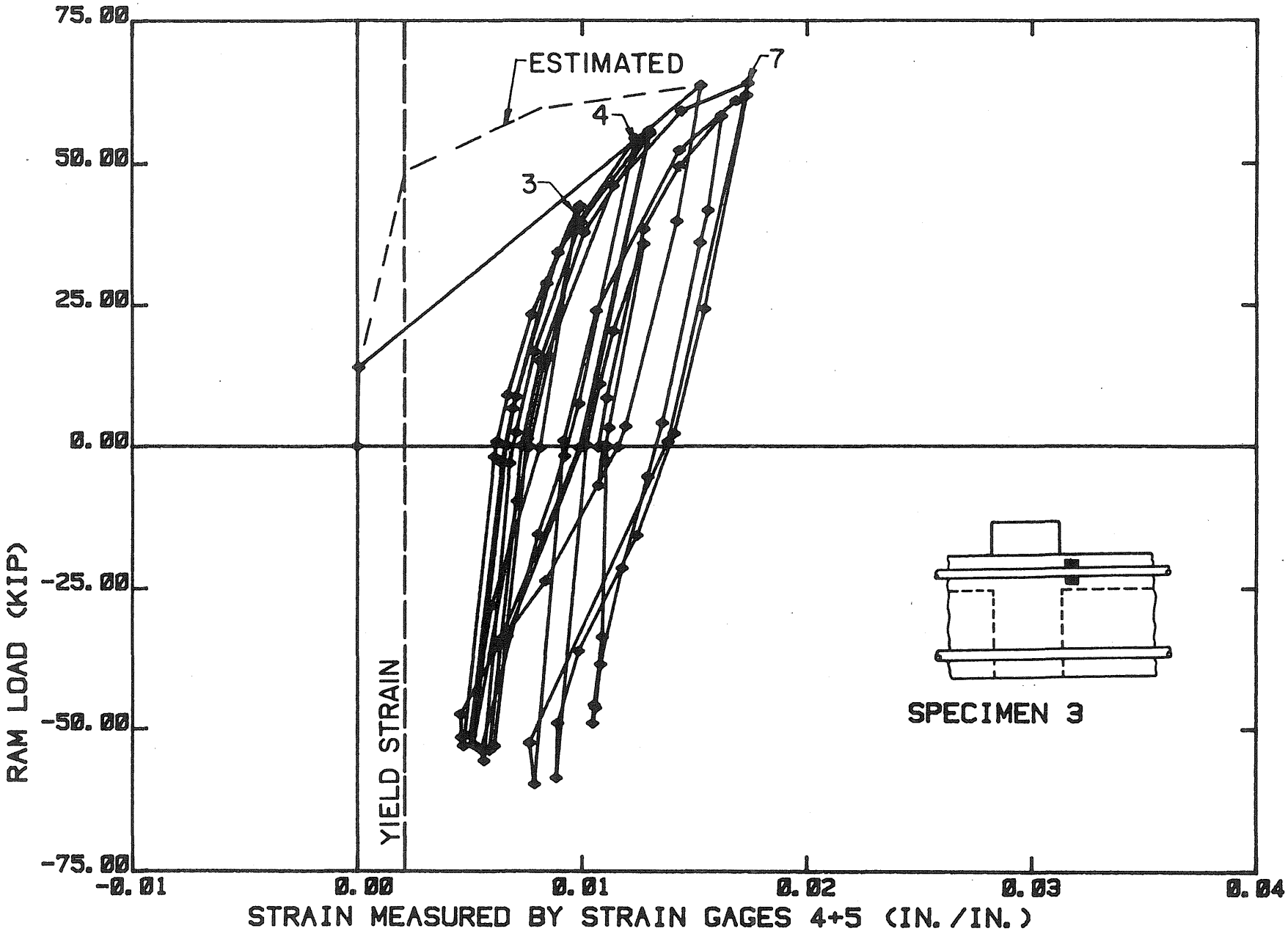

Fig. 3.2c Ram Load vs. Strain in Top Steel--Specimen 3

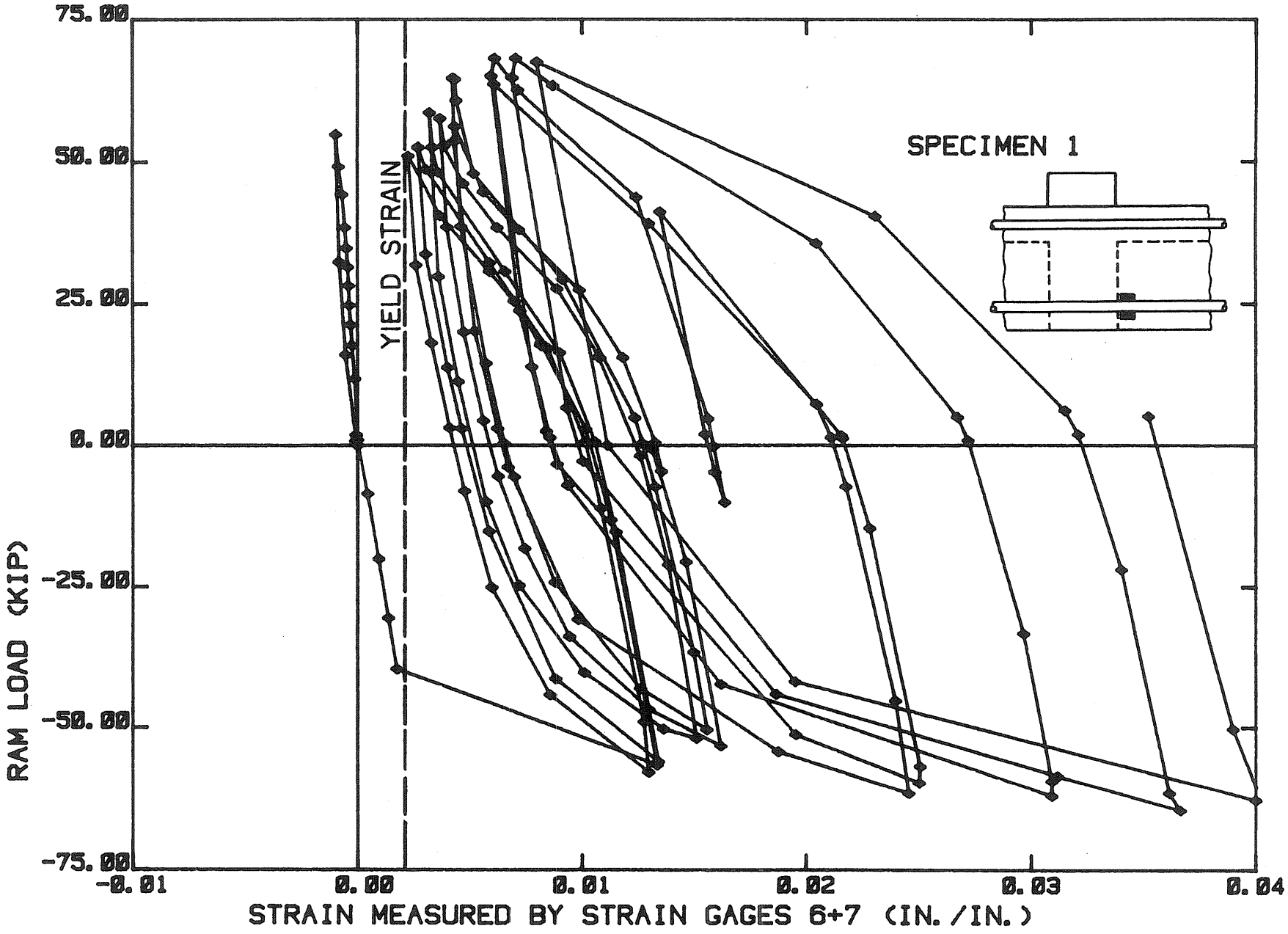

Fig. 3.3a Ram Load vs. Strain in Bottom Steel--Specimen 1

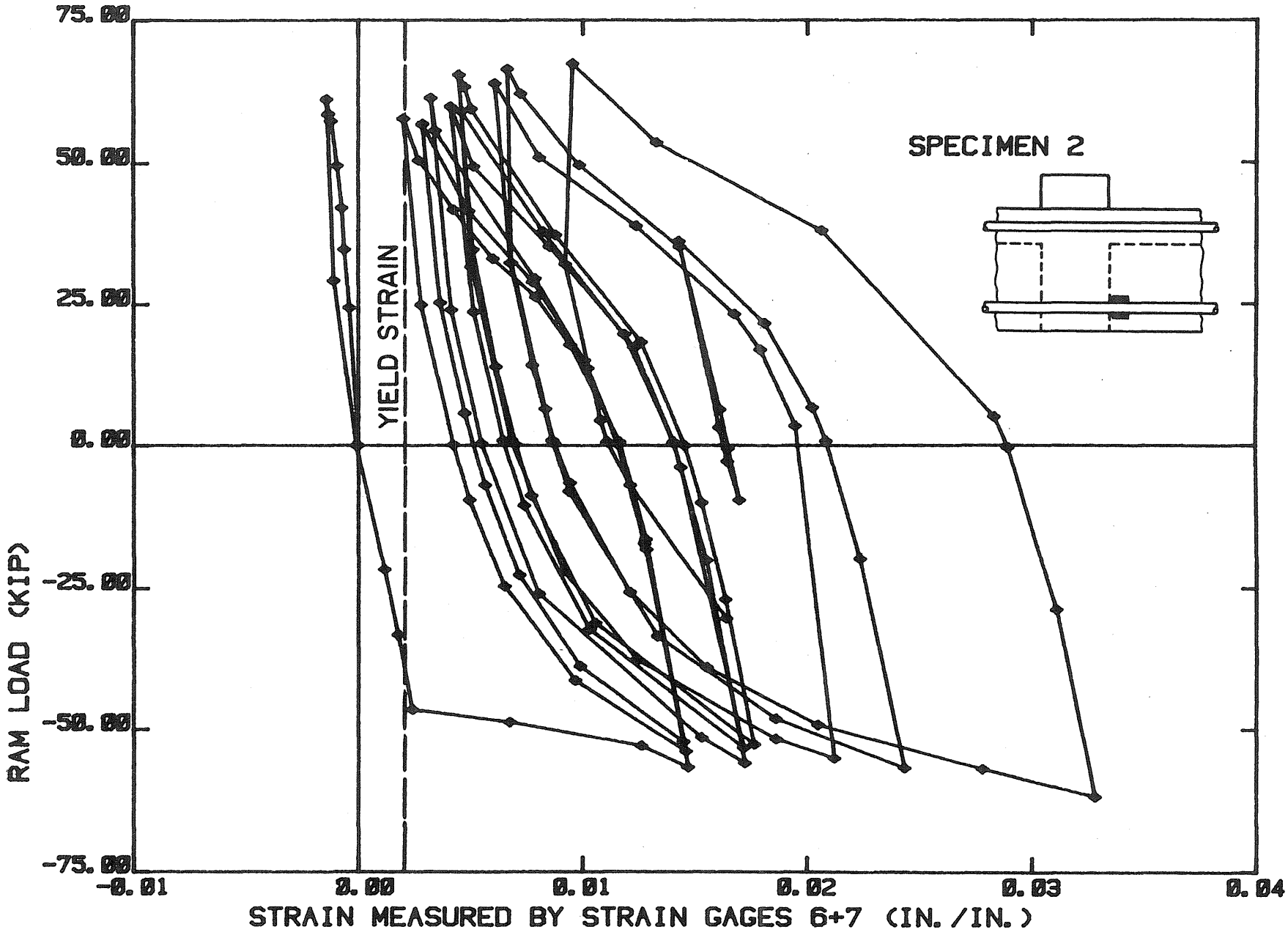

Fig. 3.3b Ram Load vs. Strain in Bottom Steel--Specimen 2

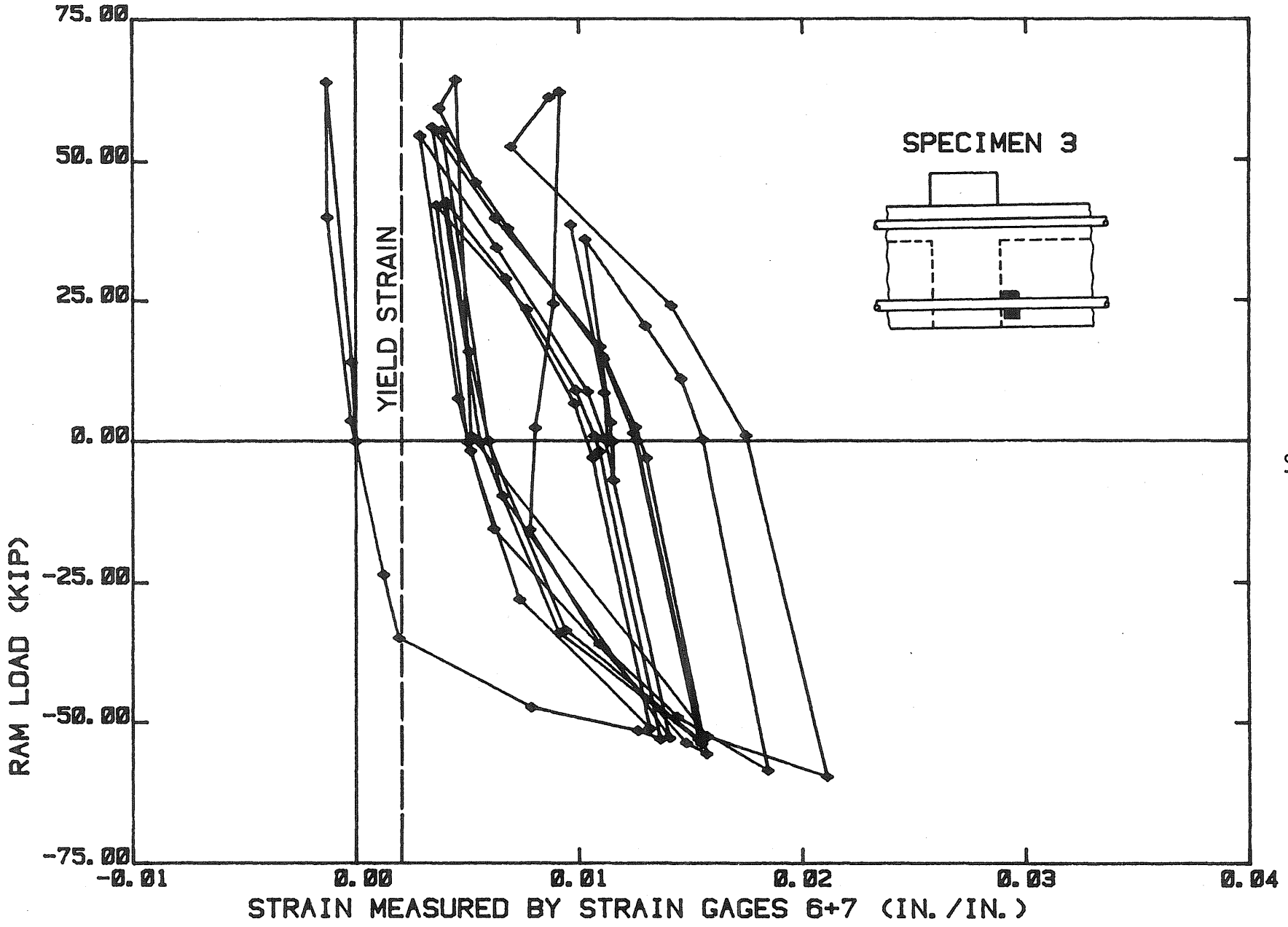

Fig. 3.3c Ram Load vs. Strain in Bottom Steel--Specimen 3

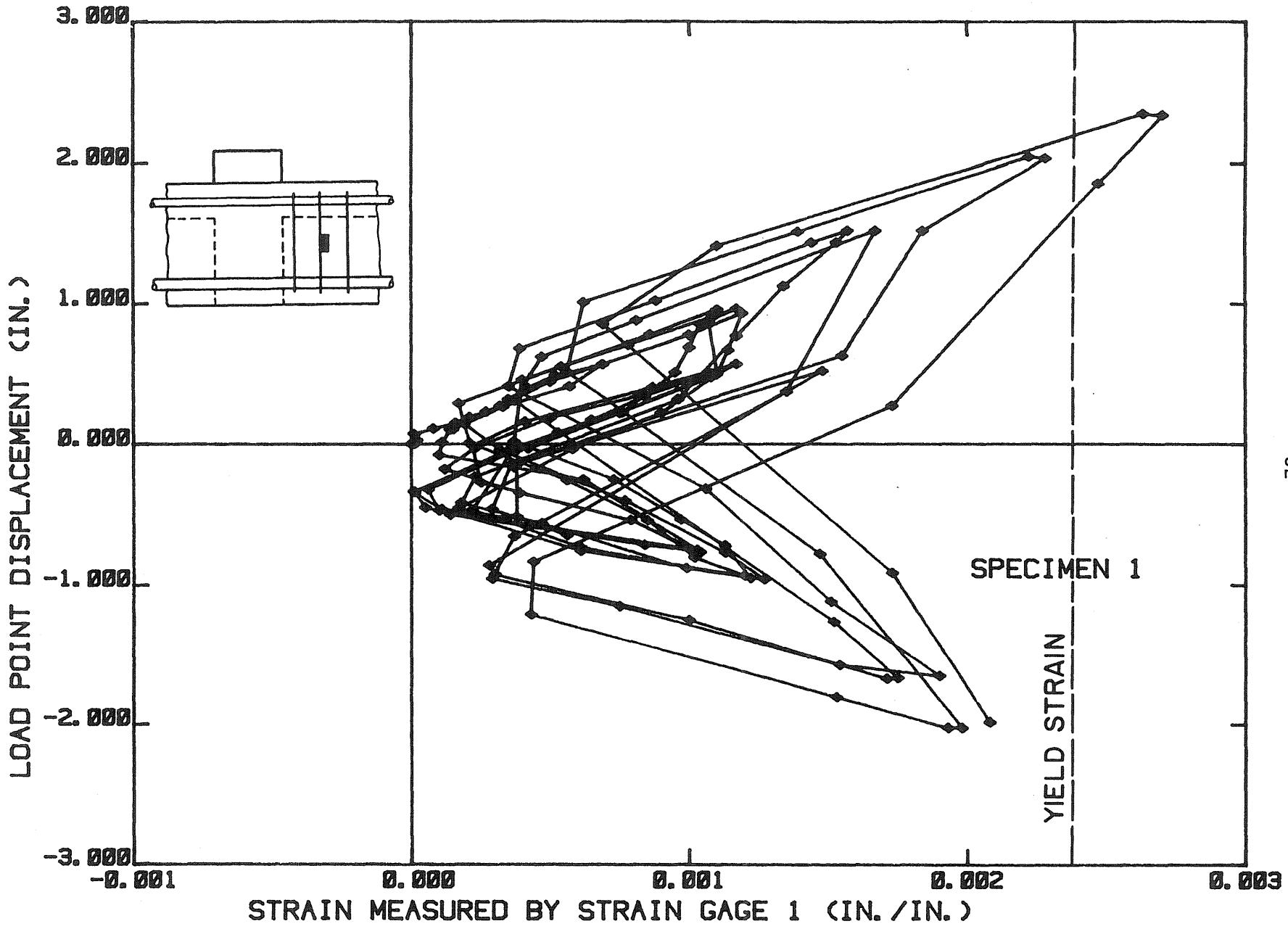

Fig. 3.4a Center Displacement vs. Strain in Stirrup--Gage 1, Specimen 1

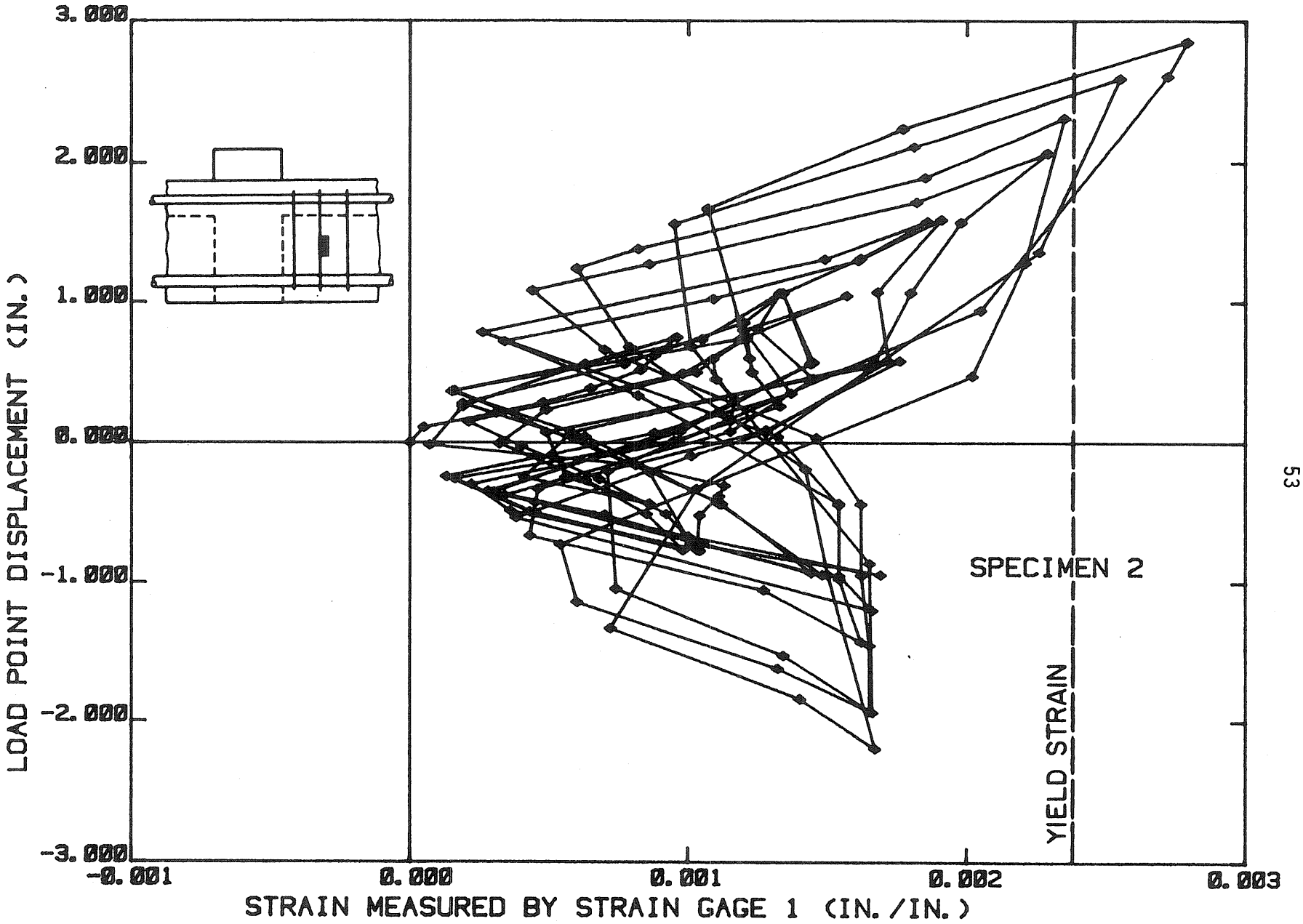

Fig. 3.4b Center Displacement vs. Strain in Stirrup--Gage 1, Specimen 2

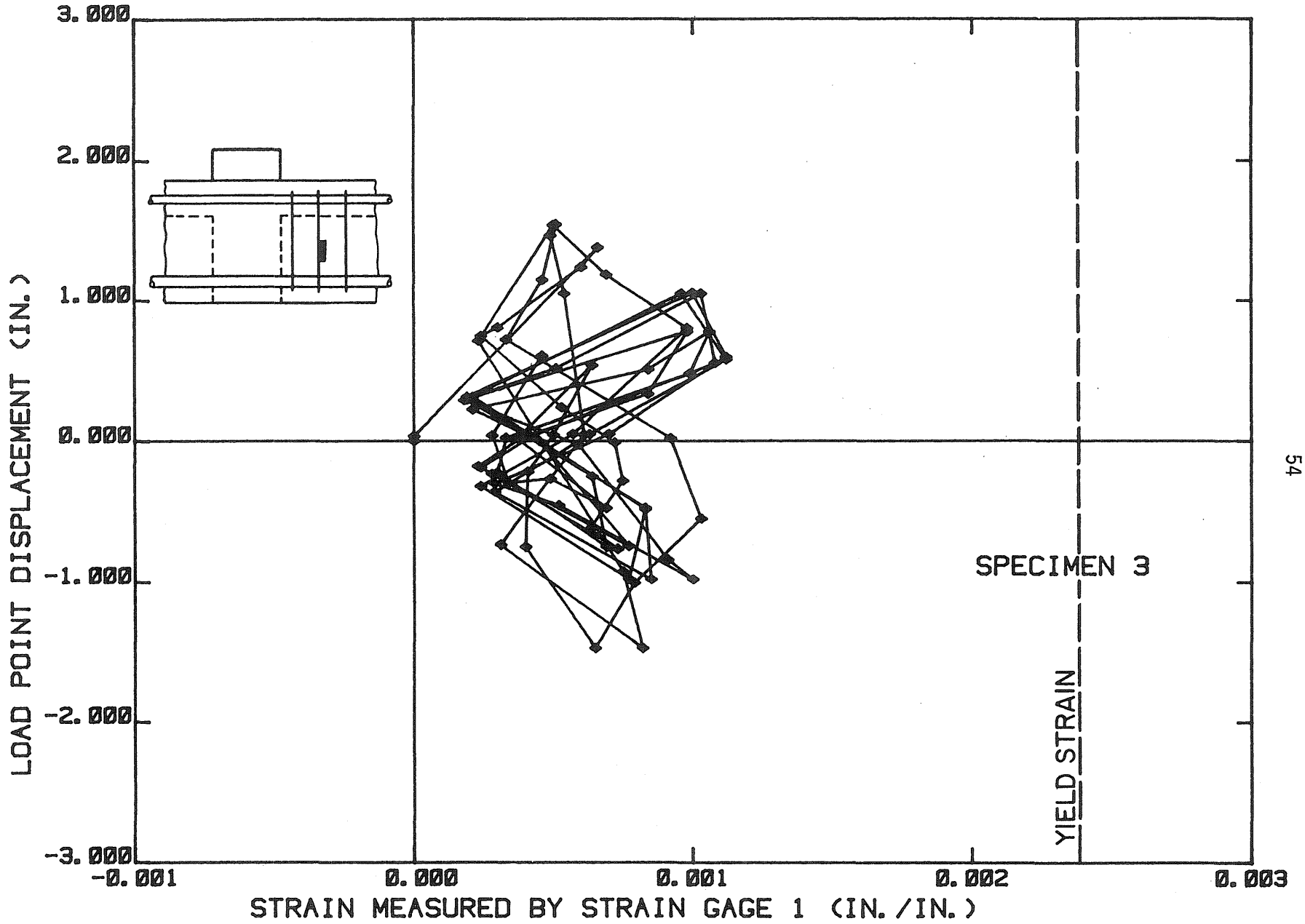

Fig. 3.4c Center Displacement vs. Strain in Stirrup--Gage 1, Specimen 3

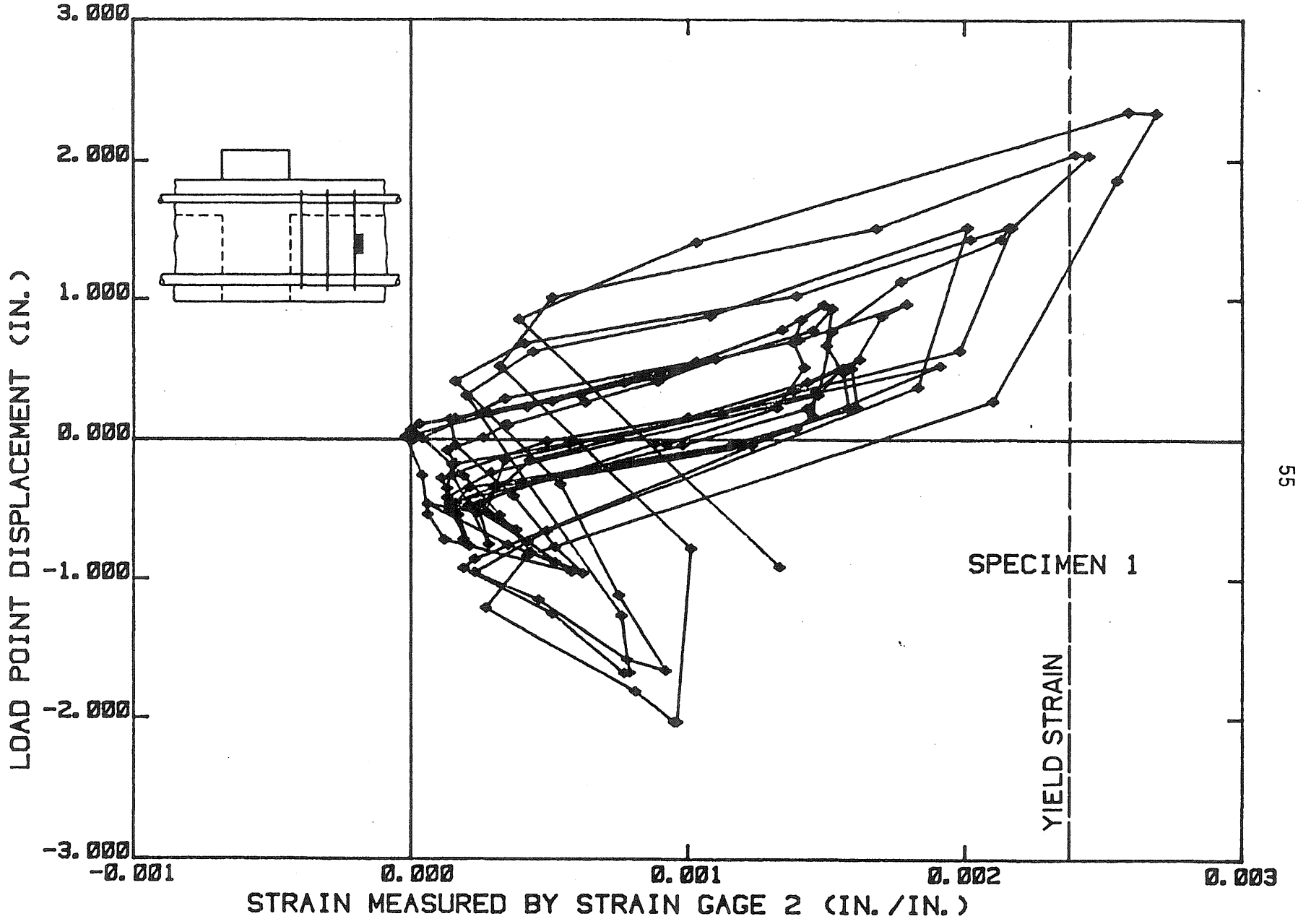

Fig. 3.5a Center Displacement vs. Strain in Stirrup--Gage 2, Specimen 1

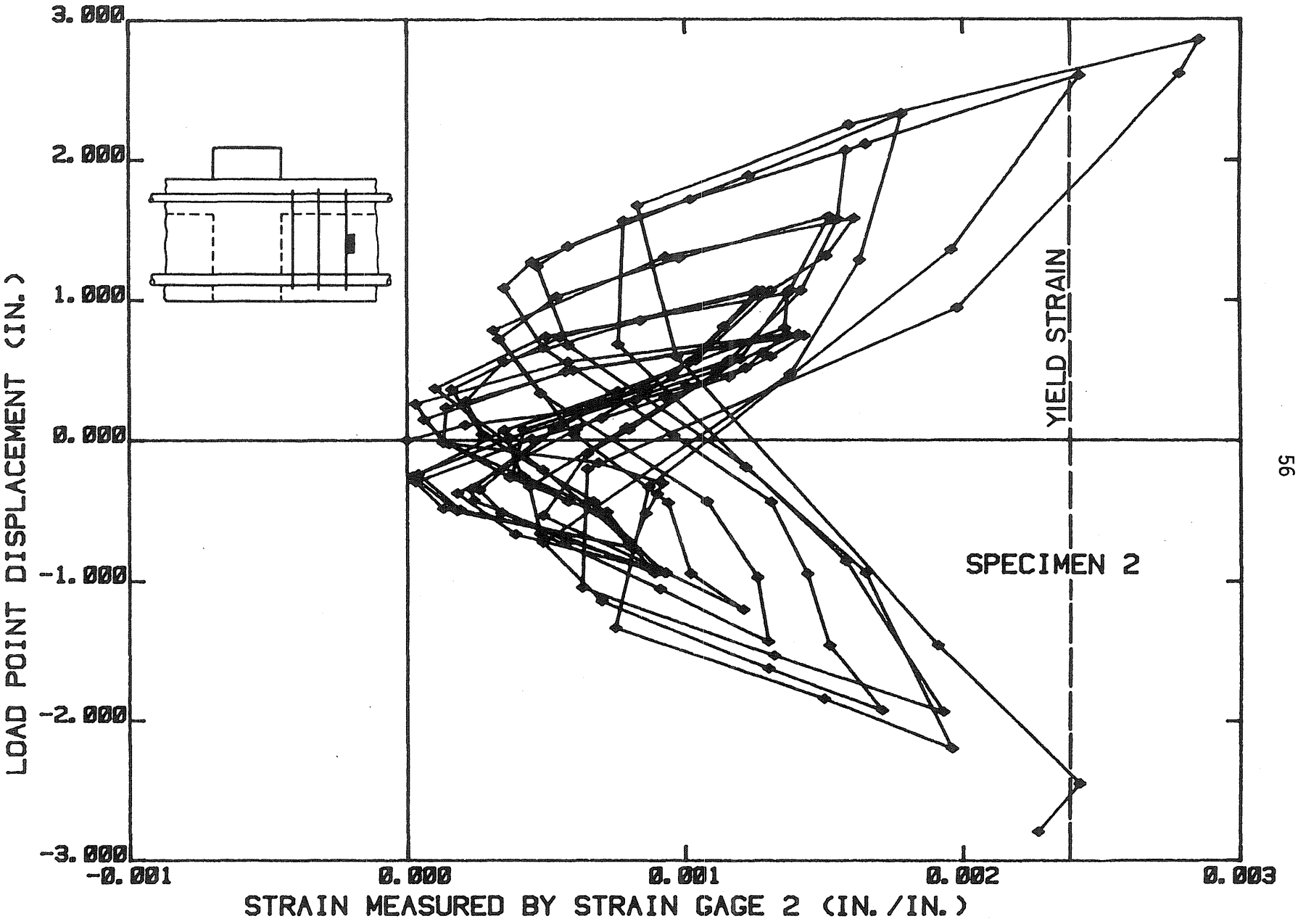

Fig. 3.5b Center Displacement vs. Strain in Stirrup--Gage 2, Specimen 2

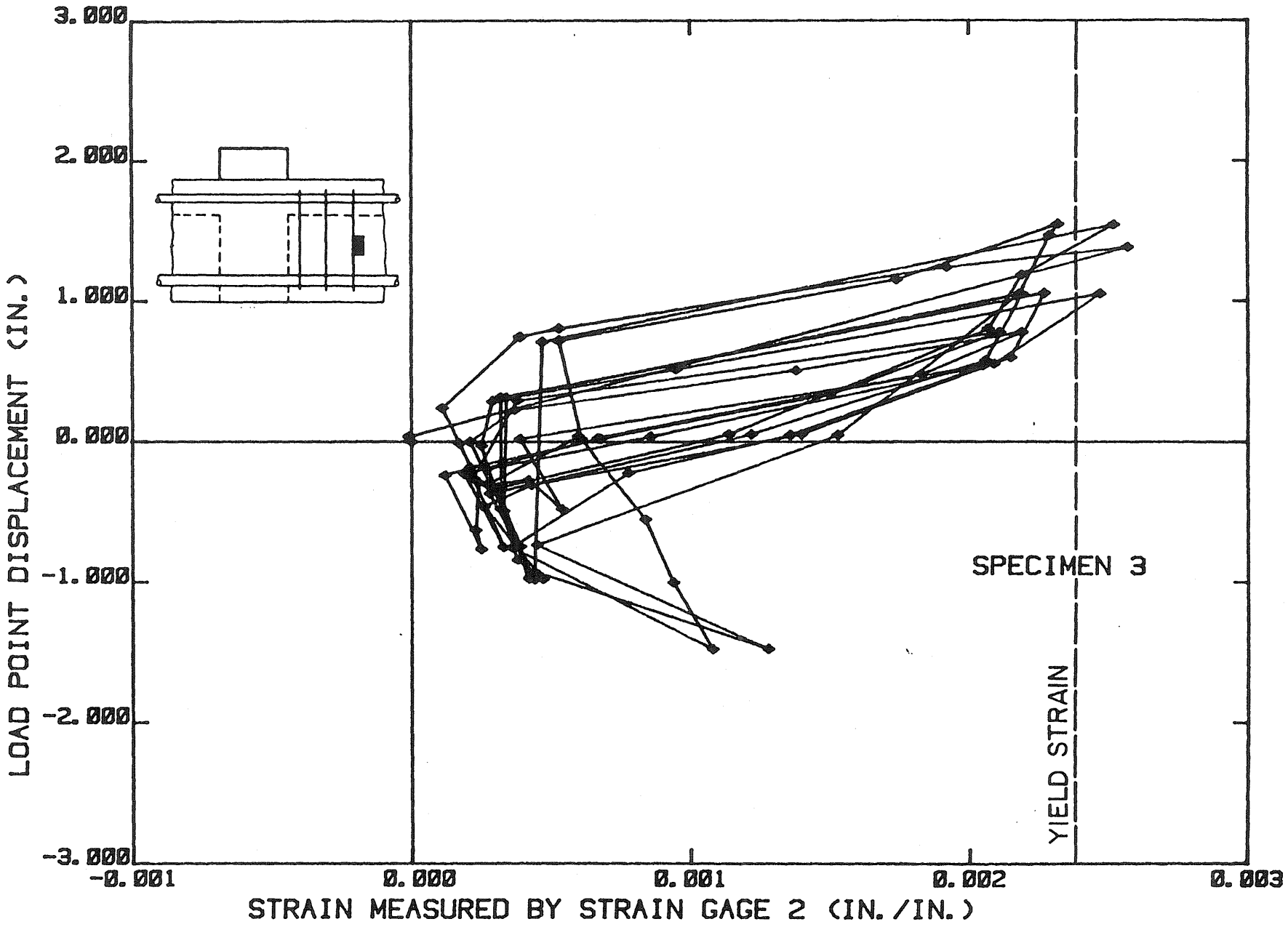

Fig. 3.5c Center Displacement vs. Strain in Stirrup--Gage 2, Specimen 3

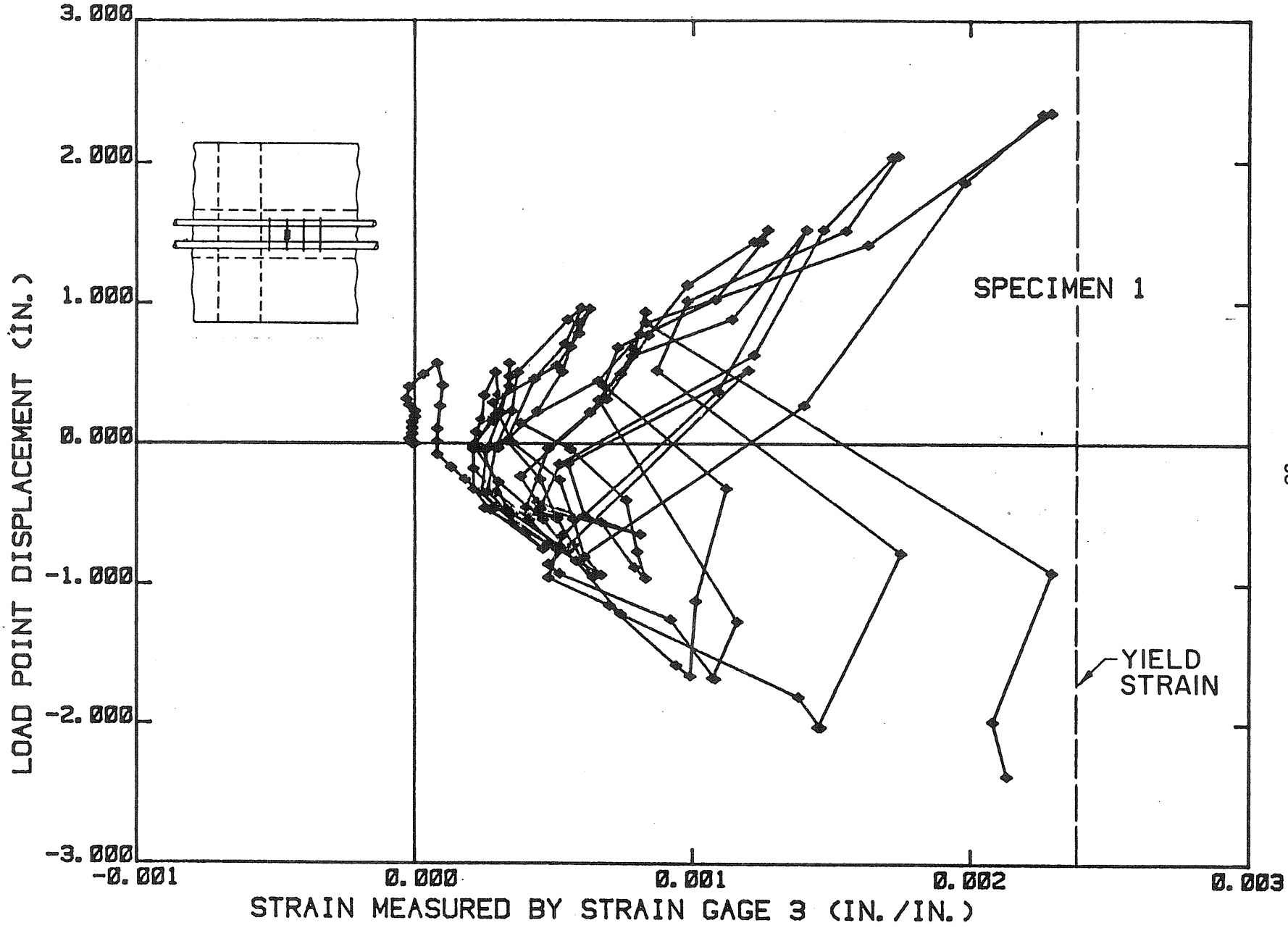

Fig. 3.6a Center Displacement vs. Flange Lateral Strain--Specimen 1

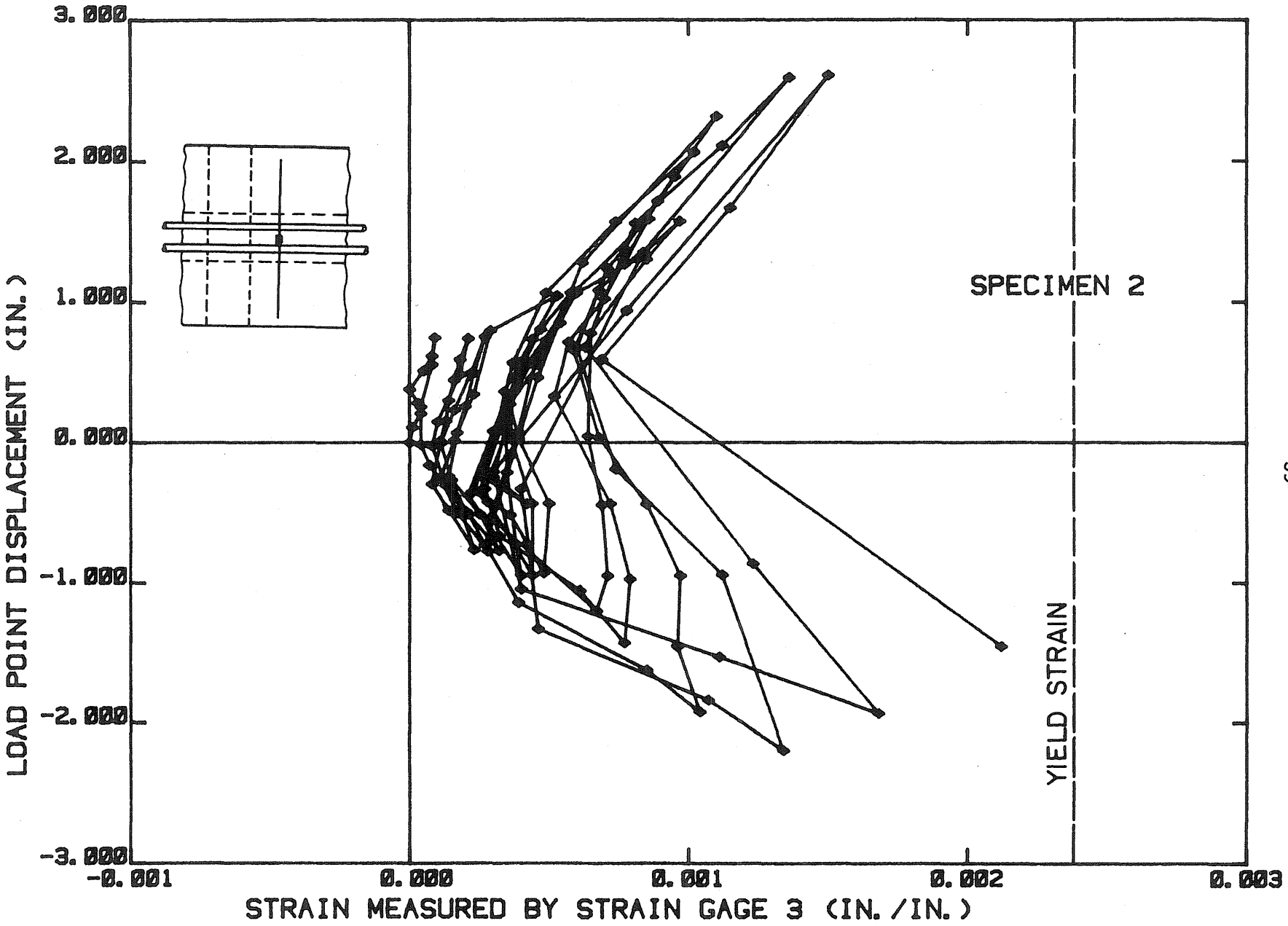

Fig. 3.6b Center Displacement vs. Flange Lateral Strain--Specimen 2

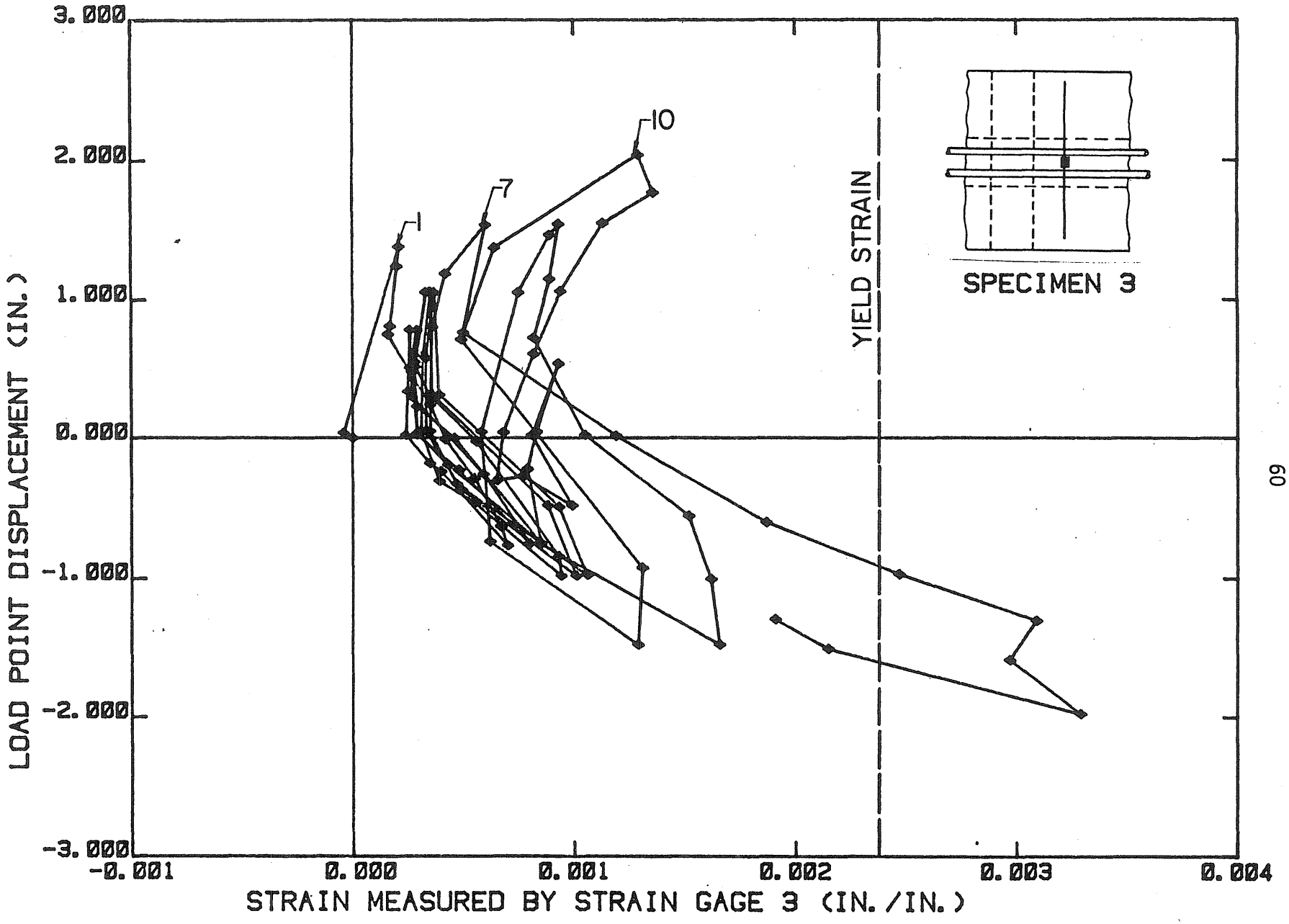

Fig. 3.6c Center Displacement vs. Flange Lateral Strain--Specimen 3

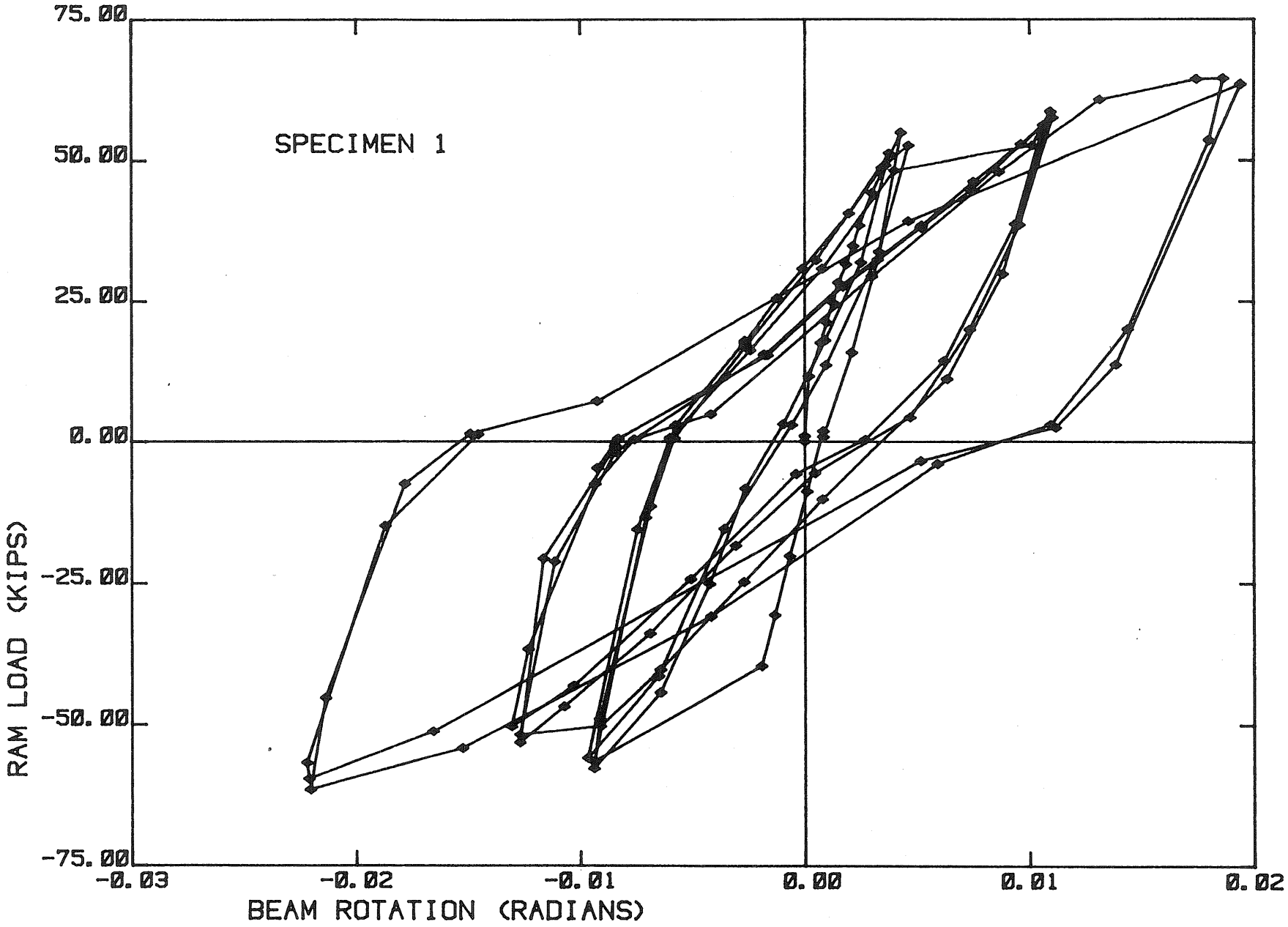

Fig. 3.7a Ram Load vs. Beam Rotation--Specimen 1

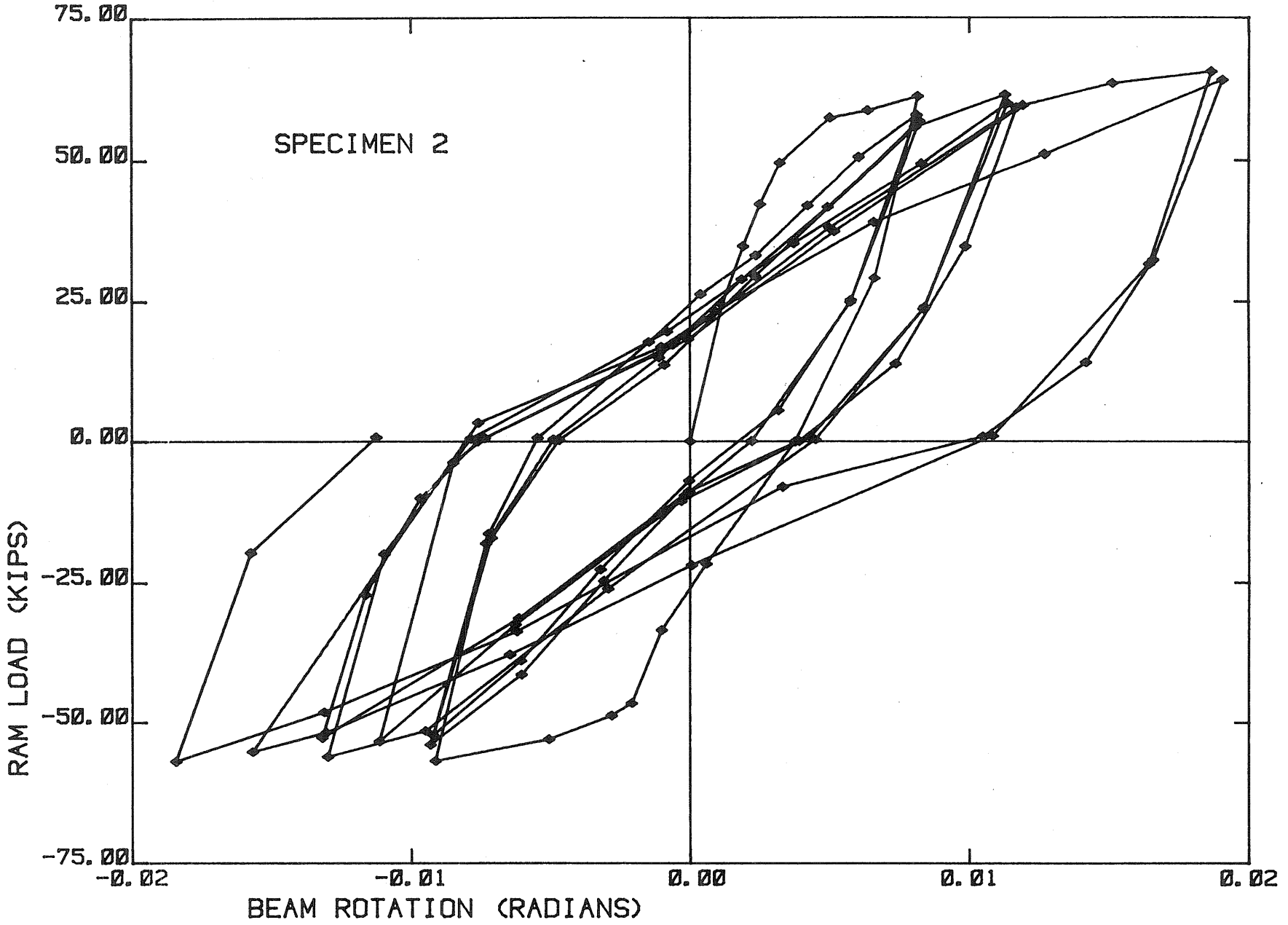

Fig. 3.7b Ram Load vs. Beam Rotation--Specimen 2

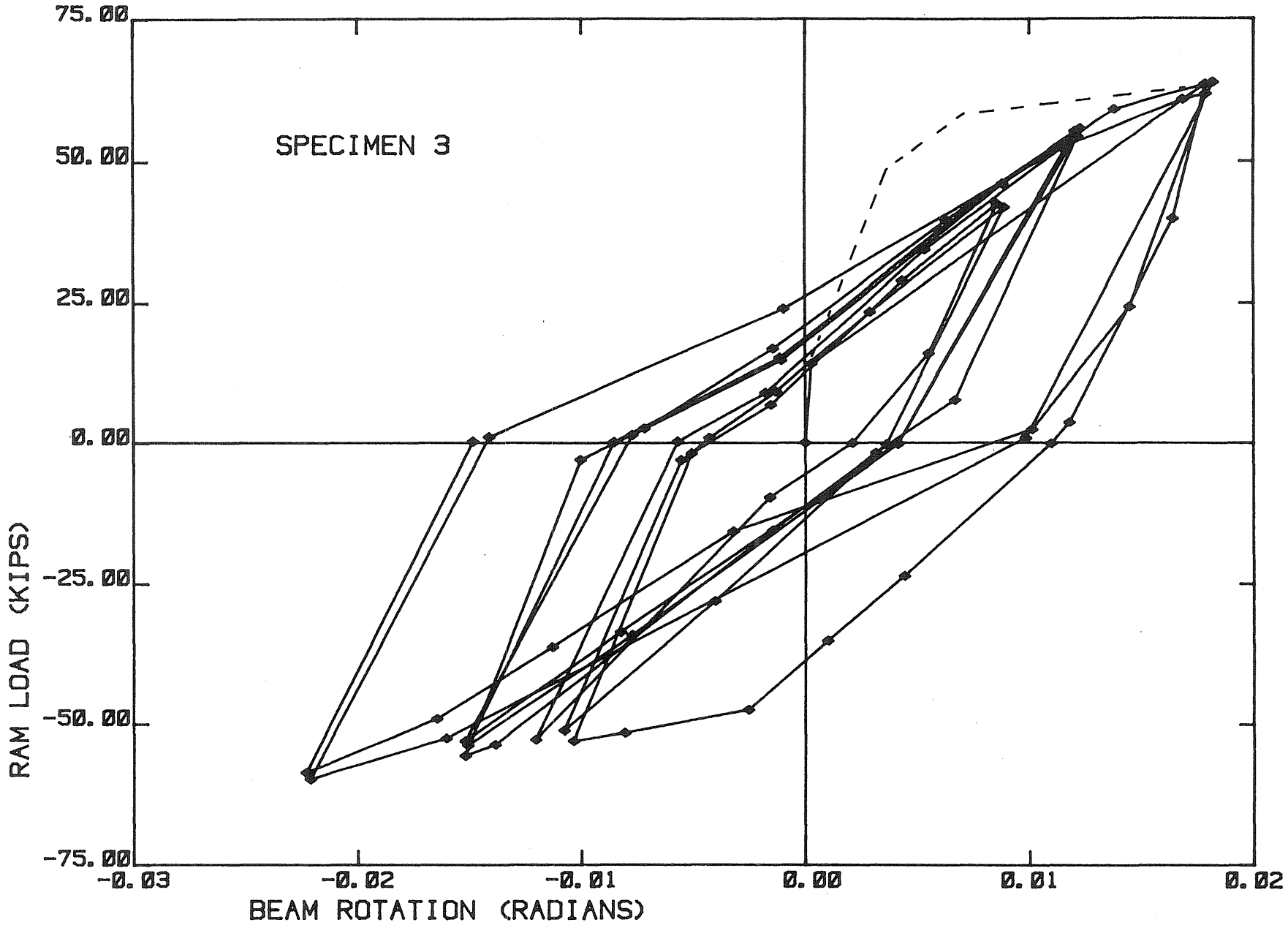

Fig. 3.7c Ram Load vs. Beam Rotation--Specimen 3

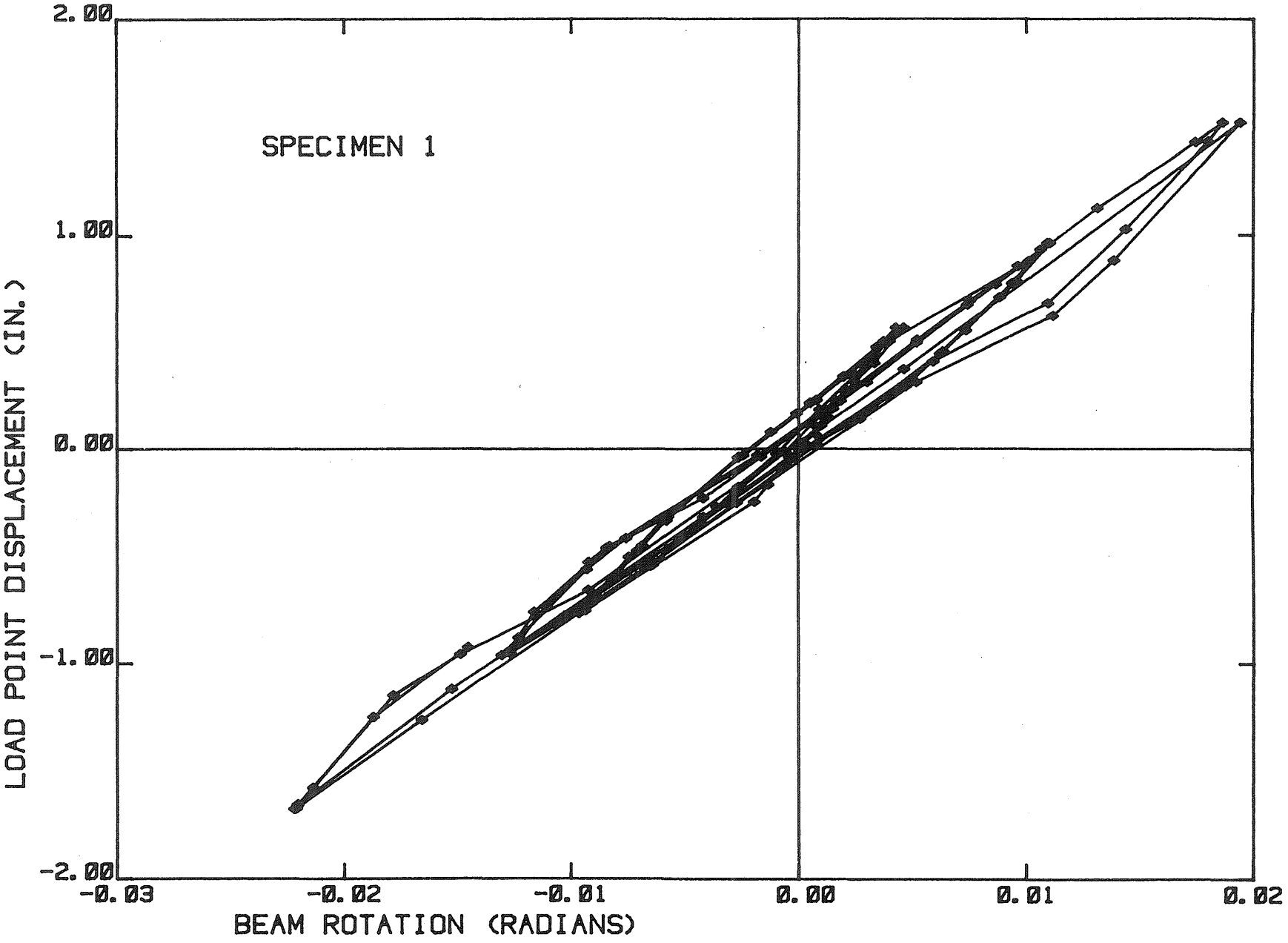

Fig. 3.8a Center Displacement vs. Beam Rotation--Specimen 1

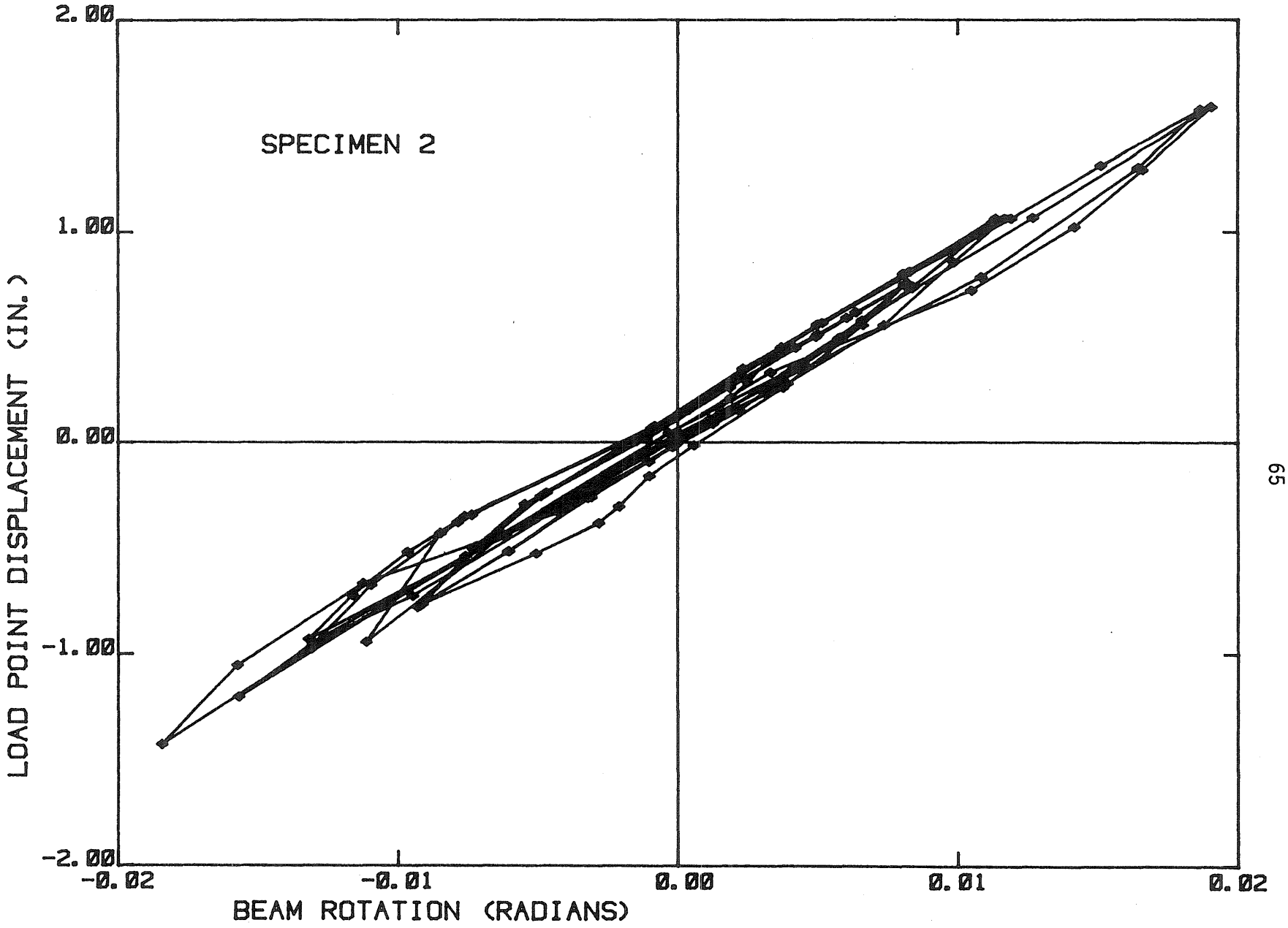

Fig. 3.8b Center Displacement vs. Beam Rotation--Specimen 2

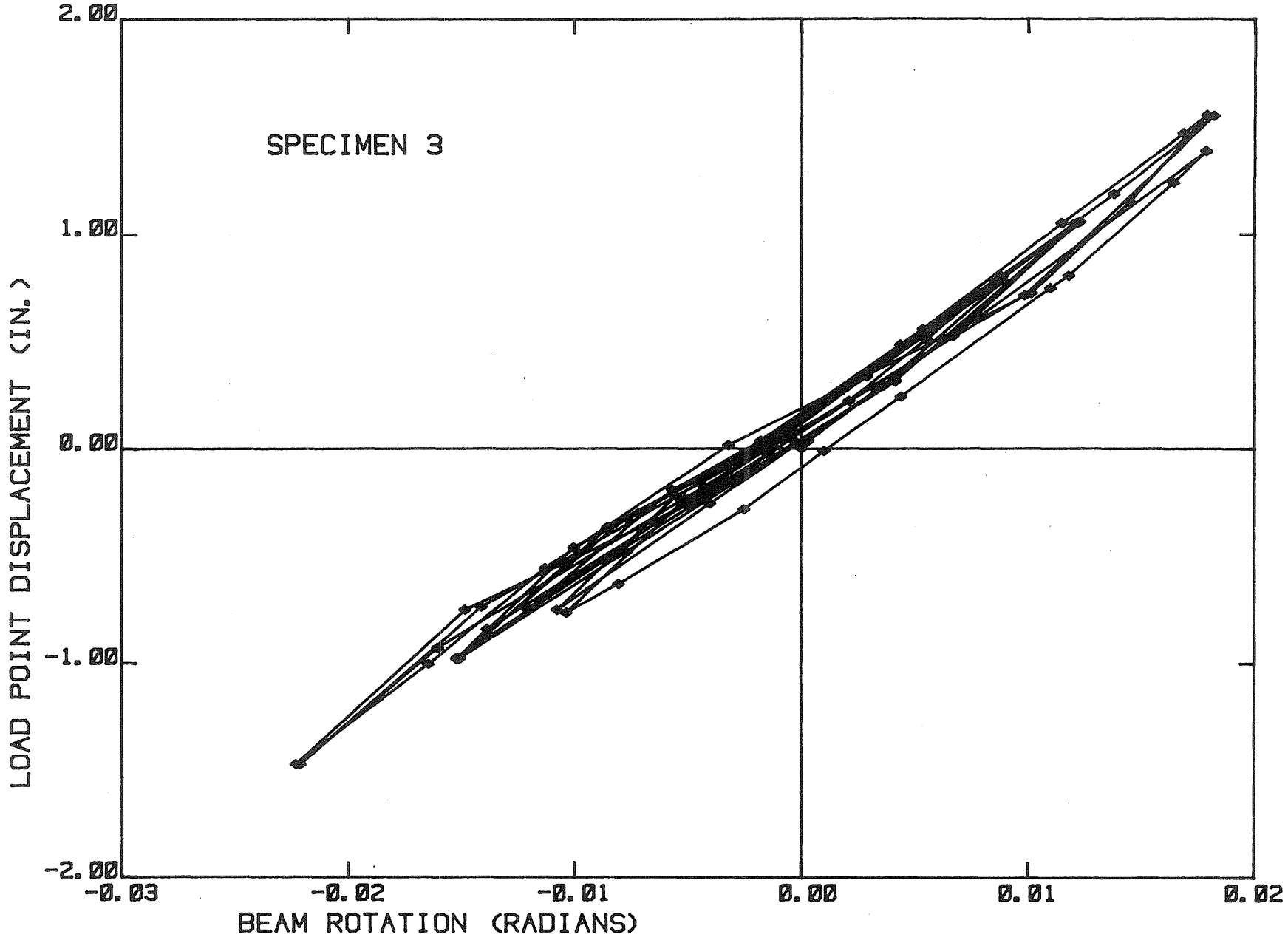

Fig. 3.8c Center Displacement vs. Beam Rotation--Specimen 3

(a) During First Half-Cycle

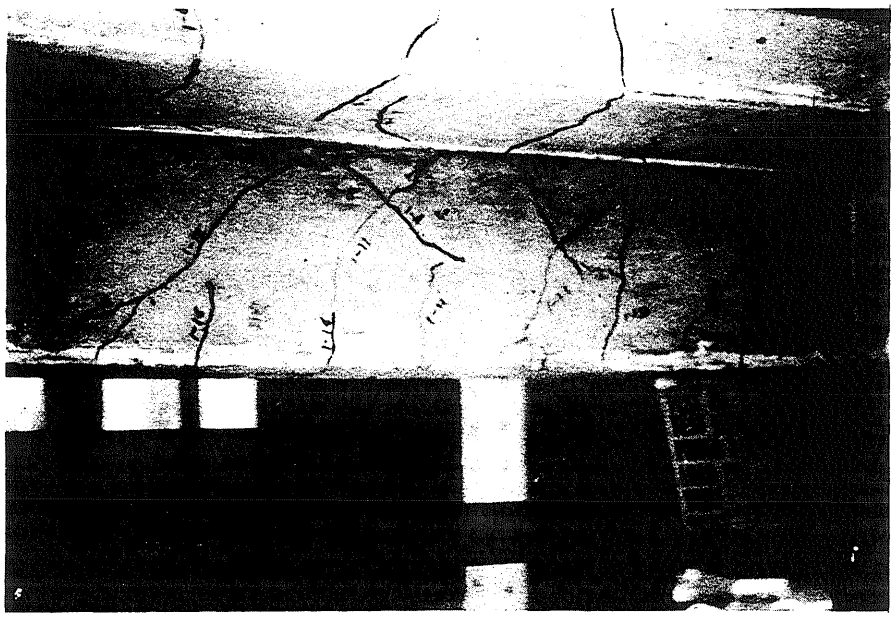

(b) During Second Half-Cycle

Fig. 3.9 Crack Patterns in Specimen 2

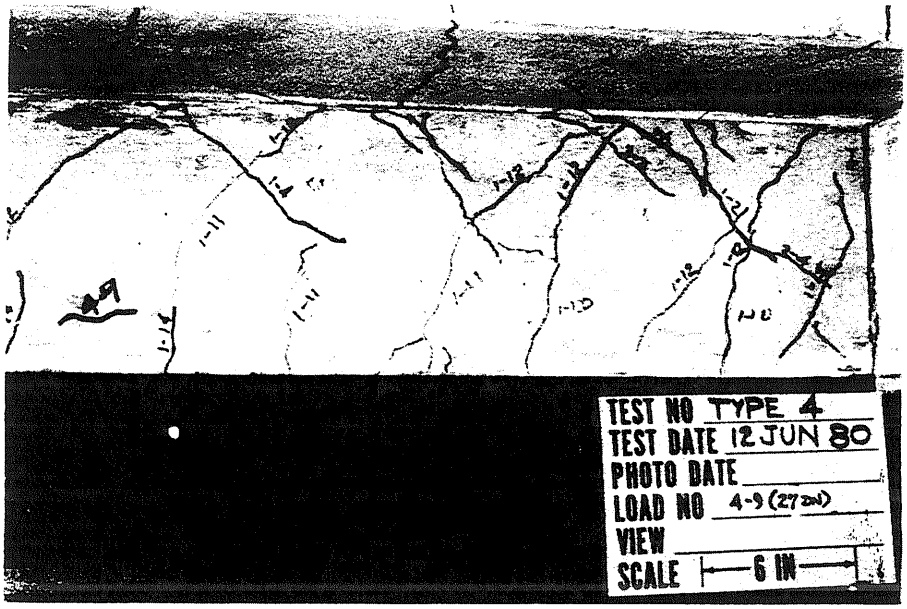

(a) Following Fourth Load Cycle

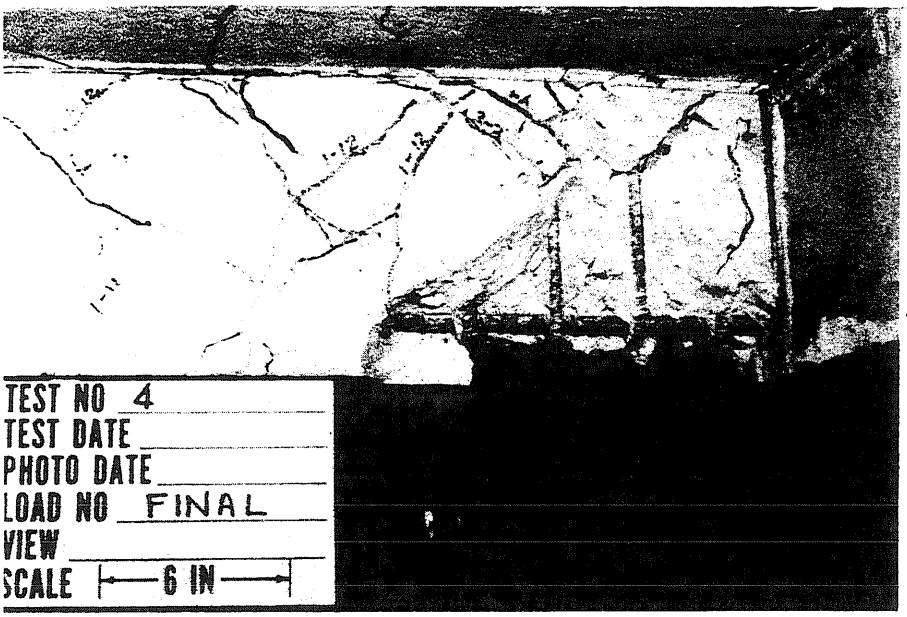

(b) At Failure

Fig. 3.10 Crack Patterns in Specimen 2

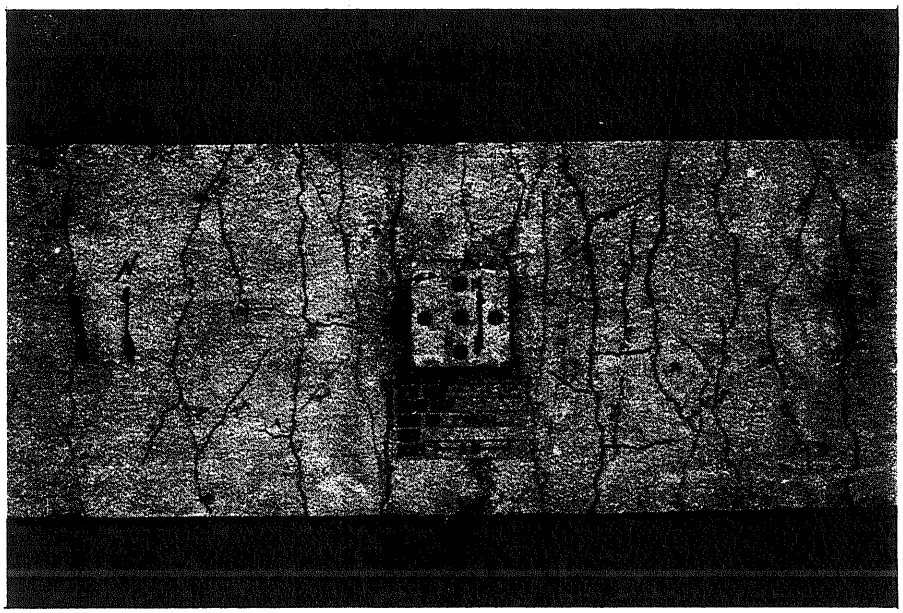

(a) Specimen 2

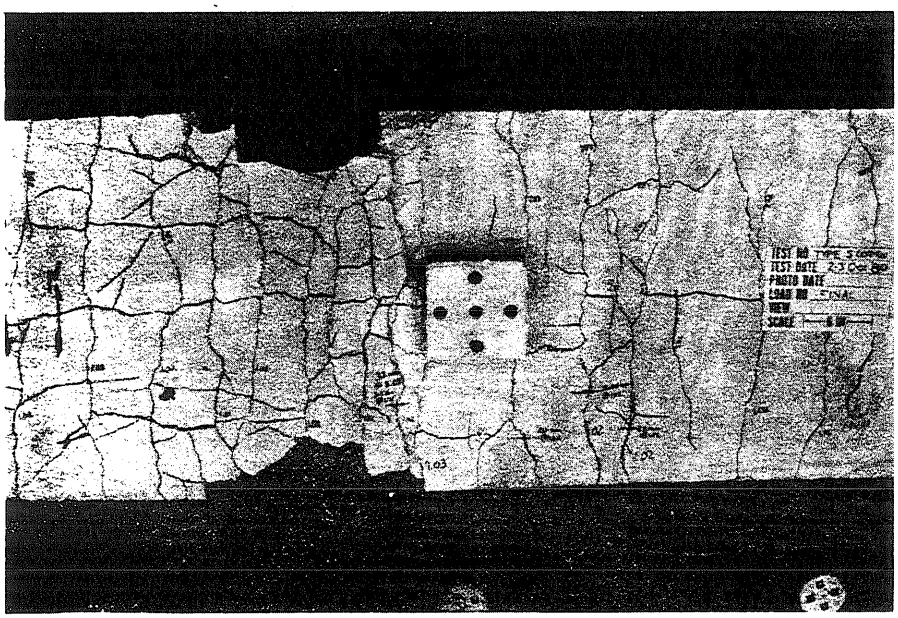

(b) Specimen 3

Fig. 3.11 Flange Crack Patterns at Failure

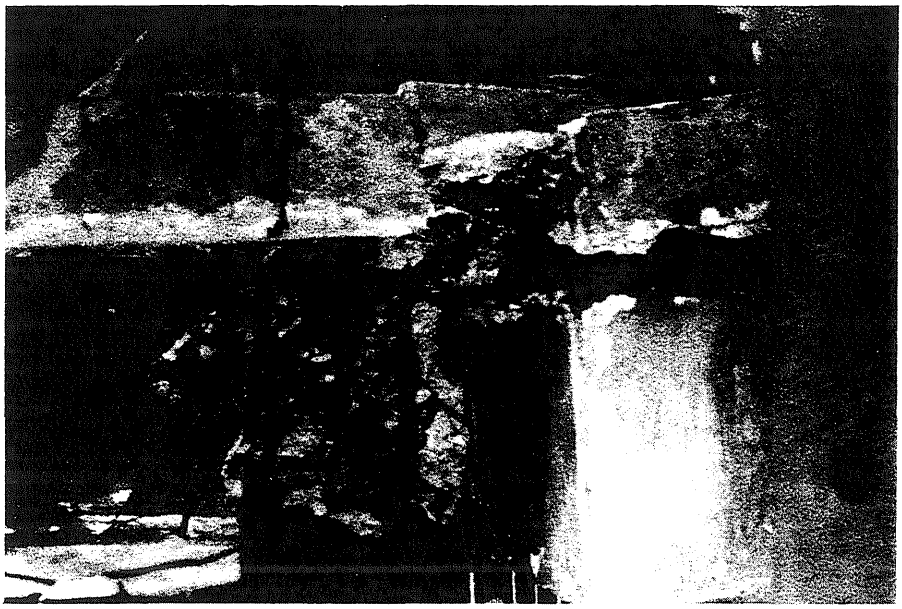

(a) Southwest side of Crossbeam

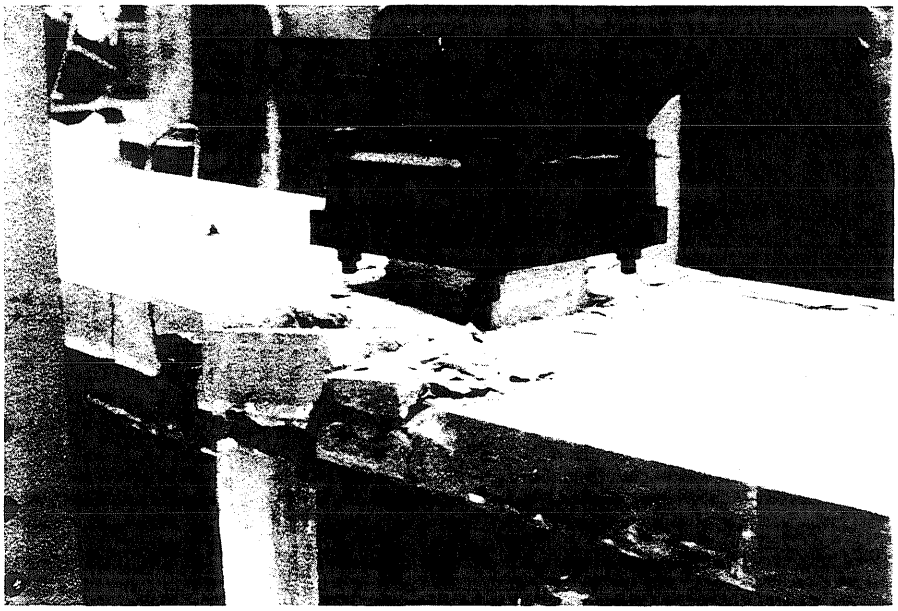

(b) Southeast Side

Fig. 3.12 Specimen 1 at Failure

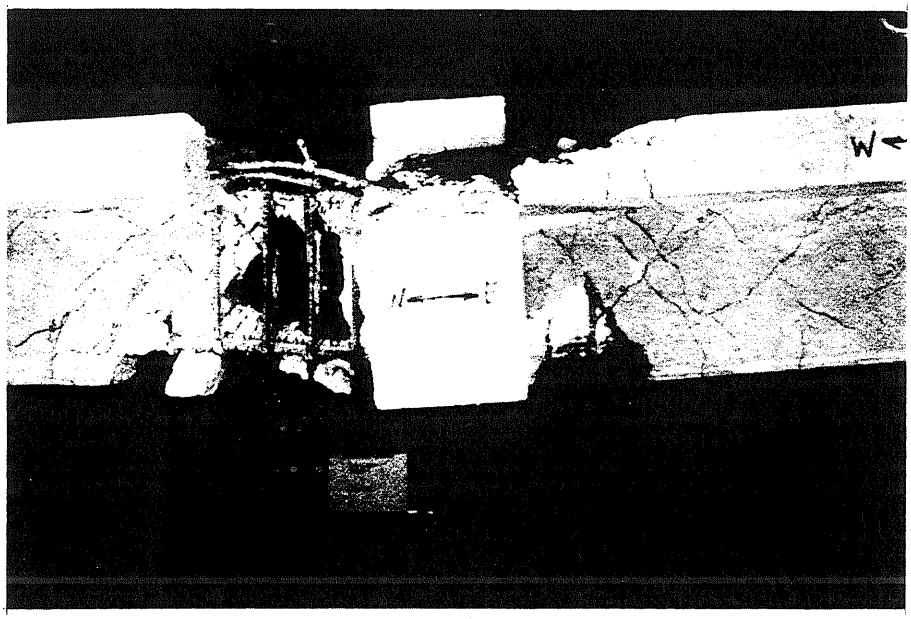

(a) Specimen 1 - Loose Concrete Removed

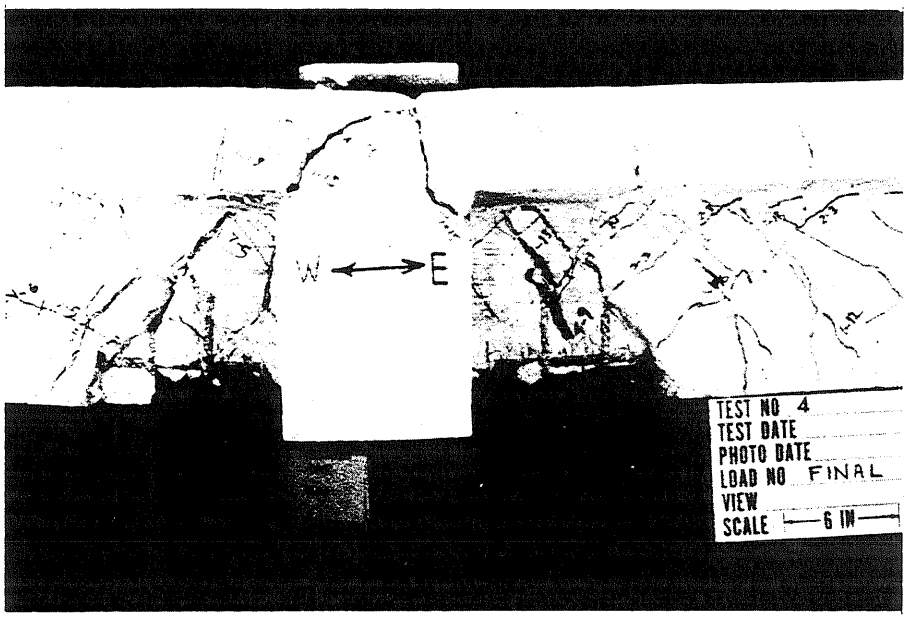

(b) Specimen 2

Fig. 3.13 Specimens 1 and 2 at Failure

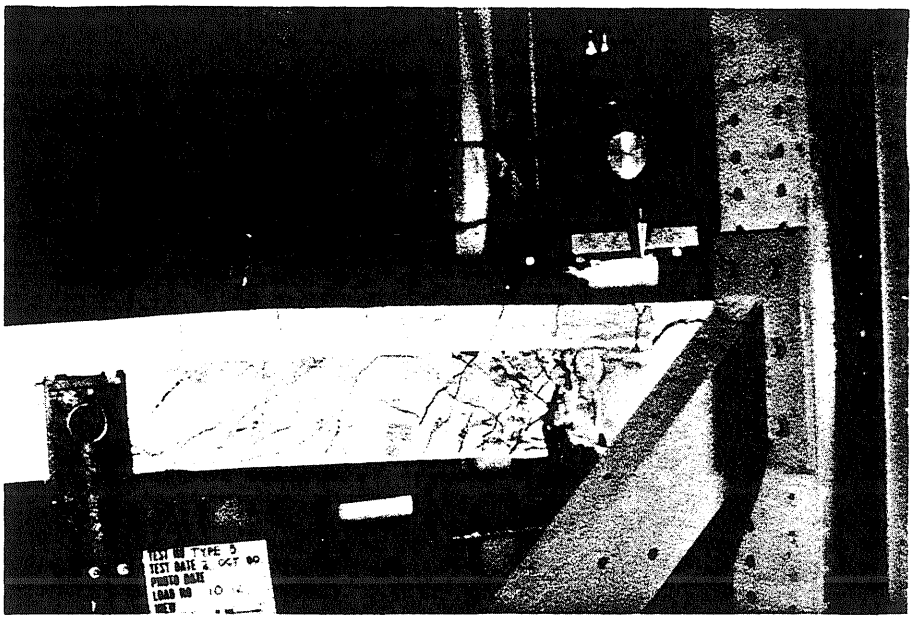

(a) During Cycle 10

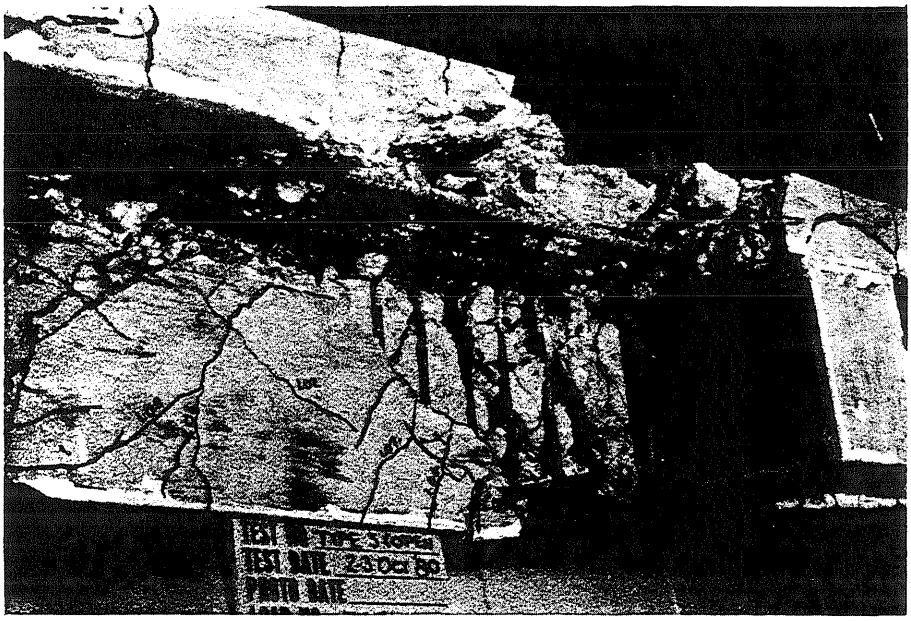

(b) View Showing Stirrup Loss of Anchorage

Fig. 3.14 Views of Specimen 3 at Failure